

1 **Title:** Individual identity information persists in learned calls of introduced parrot populations

2

3 **Authors:** Grace Smith-Vidaurre^{1,2,3,4,*}, Valeria Pérez-Marrufo^{1,5}, Elizabeth A. Hobson⁴,
4 Alejandro Salinas-Melgoza⁶, Timothy F. Wright¹

5

6 **Affiliations:**

7 ¹Department of Biology, New Mexico State University, Las Cruces, New Mexico, U.S.A.

8 ²Laboratory of Neurogenetics of Language, Rockefeller University, New York, New York,
9 U.S.A.

10 ³Rockefeller University Field Research Center, Millbrook, New York, U.S.A.

11 ⁴Department of Biological Sciences, University of Cincinnati, Cincinnati, Ohio, U.S.A.

12 ⁵Department of Biology, Syracuse University, Syracuse, New York, U.S.A.

13 ⁶Facultad de Biología, Universidad Michoacana de San Nicolás de Hidalgo, Morelia,
14 Michoacán, Mexico

15

16 * gsvidaurre@gmail.com

17

18 **Abstract**

19 Animals can actively encode different types of identity information in learned communication
20 signals, such as group membership or individual identity. The social environments in which
21 animals interact may favor different types of information, but whether identity information
22 conveyed in learned signals is robust or responsive to social disruption over short
23 evolutionary timescales is not well understood. We inferred the type of identity information
24 that was most salient in vocal signals by combining computational tools, including supervised
25 machine learning, with a conceptual framework of “hierarchical mapping”, or patterns of
26 relative acoustic convergence across social scales. We used populations of a vocal learning
27 species as a natural experiment to test whether the type of identity information emphasized in
28 learned vocalizations changed in populations that experienced the social disruption of
29 introduction into new parts of the world. We compared the social scales with the most salient
30 identity information among native and introduced range monk parakeet (*Myiopsitta*
31 *monachus*) calls recorded in Uruguay and the United States, respectively. We also evaluated

32 whether the identity information emphasized in introduced range calls changed over time. To
33 place our findings in an evolutionary context, we compared our results with another parrot
34 species that exhibits well-established and distinctive regional vocal dialects that are
35 consistent with signaling group identity. We found that both native and introduced range monk
36 parakeet calls displayed the strongest convergence at the individual scale and minimal
37 convergence within sites. We did not identify changes in the strength of acoustic convergence
38 within sites over time in the introduced range calls. These results indicate that the individual
39 identity information in learned vocalizations did not change over short evolutionary timescales
40 in populations that experienced the social disruption of introduction. Our findings point to
41 exciting new research directions about the robustness or responsiveness of communication
42 systems over different evolutionary timescales.

43

44 **Author summary**

45 In some avian and mammalian lineages, vocal communication partially depends on social
46 learning. Learned vocalizations may carry information important to communicate to others,
47 including individual identity or group membership. The information encoded in learned
48 vocalizations may change under different social conditions, such as the number of individuals
49 available for social interactions. We used populations of monk parakeets introduced to the
50 United States of America as a natural experiment of social disruption. We tested the ideas
51 that the type of identity information encoded in learned vocalizations could either remain the
52 same or change in introduced populations compared to native range populations in Uruguay.
53 Using computational approaches, we quantified patterns of acoustic variation linked to identity
54 information in learned vocalizations of native and introduced range populations. We found
55 that individual identity information was more pronounced than group membership in learned
56 vocalizations in each of the native and introduced ranges. The type of identity information

57 important for monk parakeets to communicate appears to have remained the same despite
58 social disruption that occurred over the last 50 years. While socially learned traits are
59 considered very flexible, our findings suggest that the type of identity information encoded in
60 learned vocalizations can be robust to population disruption over cultural timescales.

61

62 **1. Introduction**

63 Animals can use communication signals to transmit social information, including group
64 membership, individual identity, social status, sex, or other social characteristics [1,2]. The
65 types of identity information that animals encode in signals may be an outcome of differences
66 in the social environment within or among species. Different types of information may be more
67 or less important for animals to communicate in social environments that can change over
68 ecological or evolutionary timescales [3–6].

69 Vocalizations are well-studied communication signals that can contain identity
70 information. For example, voice cues arising from vocal tract filtering can provide receivers
71 with information about individual identity [7–9]. However, individuals can also use social
72 learning to modify identity information, such as vocal learning species that can encode both
73 group-level and individual identity information in learned vocalizations in a stable manner.
74 When individuals imitate vocalizations of their social companions, the resulting group-level
75 acoustic convergence can be used to recognize group members [10–12]. Learned
76 vocalizations with group identity information, such as vocal dialects, have been reported in
77 several vocal learning taxa, including cetaceans [13–17], bats [18], songbirds [19–21], and
78 parrots [22,23]. Individuals can also communicate individual identity information by developing
79 distinctive vocalizations that differentiate them from other individuals. For instance, bottlenose
80 dolphins (*Tursiops truncatus*) and green-rumped parrotlets (*Forpus passerinus*) can use vocal

81 learning to produce distinctive individual signatures used for individual vocal recognition [24–
82 27].

83 These findings from the same or closely related taxa suggest that changes in the social
84 environment could influence the identity information that animals encode in learned
85 vocalizations. For instance, living in large social groups or interacting repeatedly with different
86 individuals may favor signaling individual identity information, due to either the pressure of
87 providing sufficient information for receivers to discriminate among unique individuals [28], or
88 the relative benefits and costs associated with maintaining many different social relationships
89 [29]. However, the degree to which identity information encoded in learned communication
90 signals dynamically responds to changes in social conditions over short evolutionary
91 timescales is not well understood.

92 Short-term changes in the social environment can influence variation within or among
93 types of identity information in learned vocalizations, which could reflect novel changes to the
94 identity information used, or switching among historical forms of identity signaling. For
95 instance, captive and wild Puerto Rican Amazon parrots (*Amazona vittata*) exhibit distinct
96 vocal dialects that have arisen over only a few decades, and translocated individuals will
97 switch between dialects to call in the dialect of the local population [22]. In a field experiment
98 with yellow-naped amazons (*Amazona auropalliata*), a juvenile translocated between regional
99 populations also switched to calling in the local vocal dialect [30]. However, regional dialect
100 boundaries in this species remained stable over 11 years [31], despite natural dispersal of
101 individuals across dialect boundaries [32]. In elephant seals (*Mirounga angustirostris*),
102 increasing population size appears associated with a change in the type of identity
103 information encoded in learned vocalizations over short evolutionary timescales. As
104 recovering populations grew in size over 50 years, vocal dialects were replaced by more
105 structurally complex calls that displayed greater individual distinctiveness, which may facilitate

106 male signaling in more crowded social environments [33]. In eusocial naked mole-rats
107 (*Heterocephalus glaber*), individuals learn colony-specific vocal dialects during development.
108 However, the type of identity information emphasized in learned vocalizations appears
109 sensitive to social stability conferred by the presence of a queen. In a colony that lost two
110 queens within a year, individuals' chirps became less colony-specific and more individually
111 distinctive during two periods of social instability [34]. This particular change in identity
112 information may be linked to physiological mechanisms of reproductive suppression [34], but
113 still provides compelling evidence that the type of identity information encoded in learned
114 vocalizations can be sensitive to changes in social conditions within an individual's lifetime.

115 To test whether identity information in vocalizations is robust or responsive to short-
116 term changes in the social environment, we need two critical components: 1) a way to
117 quantify the relative salience of different types of identity information in learned signals and 2)
118 the potential to compare identity information across groups with different social
119 characteristics.

120 First, new tools are needed to better quantify the salient types of information in
121 vocalizations. Computational approaches like machine learning can be applied within a
122 conceptual framework that links patterns of vocal convergence to identity signaling.
123 Individuals should use vocal learning to converge on vocalizations across different scales of
124 social organization [35], and such vocal convergence should yield "hierarchical mapping"
125 patterns, which are patterns of relative acoustic convergence that vary in a stable manner
126 across social scales [1]. To evaluate hierarchical mapping patterns, we can use machine
127 learning tools to quantify relative acoustic convergence over different social scales, for
128 example, from individuals to flocks or populations inhabiting different geographic regions.
129 From hierarchical mapping patterns, we can use the social scale with the strongest relative
130 acoustic convergence to infer the most salient type of identity information encoded in

131 vocalizations. This conceptual framework assumes that patterns of acoustic convergence
132 reflect identity information encoding that is stable across social contexts, in contrast to the
133 rapid vocal matching exhibited by some vocal learners that should yield varying patterns of
134 acoustic convergence and divergence in real time [36–39].

135 Second, we can compare hierarchical mapping patterns among groups with variation in
136 population stability to test whether identity information in learned vocalizations is robust or
137 responsive to disruption of the social environment. We can leverage different types of natural
138 experiments for this comparison, including the introduction of species to new parts of the
139 world, which can cause founder effects that influence traits transmitted by genetic inheritance
140 and by social learning in introduced populations [40,41]. Introduction events that expand a
141 species' range can be an extreme form of social disruption. In particular, when this process
142 occurs through the pet trade, wild individuals are removed from their natural social
143 environments and are placed in captivity for transport, and then can remain in captivity in
144 breeding colonies that sustain the pet trade throughout the remainder of their lives. These
145 original individuals or their captive-bred descendants can also establish new populations after
146 escaping or being released from captivity [42–44]. New populations established outside of the
147 native range after this form of social disruption should be small shortly after establishment.
148 However, if population growth leads to increased population size after establishment [42],
149 then social environments that are similar to native range populations could gradually re-
150 establish in the introduced range. Alternatively, the effects of social disruption could persist
151 over generations and influence learned vocal outcomes, since vocal learning is a social
152 process. For example, there could be fewer overall numbers of individuals available for social
153 interactions in introduced populations, which could alter the cognitive costs of social
154 recognition for receivers [12,29], and in turn, alter the type of identity information that
155 signalers convey in learned vocalizations compared to the native range.

156 In this study, we focused on native and introduced range populations of monk
157 parakeets (*Myiopsitta monachus*) to test how social disruption that occurred generations ago,
158 over the course of the past 50 years, could cause changes in the type of identity information
159 encoded in contact calls. Parrots are suitable for this research because they can use social
160 learning to both acquire and modify “contact” calls, which individuals are thought to use to
161 maintain contact with their social companions while flying and foraging [45]. Monk parakeets
162 are particularly useful because they have established new populations worldwide through the
163 pet trade since the late 1960s, enabling comparisons between native range populations and
164 multiple introduced range populations. The independently established introduced range
165 populations share a common origin, with the majority of these populations stemming from
166 native range populations in Uruguay and the surrounding region of northern Argentina [46–
167 49]. In addition, we know more about monk parakeets’ social system than most parrot
168 species. While social relationships among pairs are important, experiments with captive social
169 groups indicate that this species is capable of hierarchical social organization, which could
170 extend to wild populations [50–53]. Finally, recent work has contributed to growing knowledge
171 of this species’ vocal communication system in both the native and introduced ranges [35,54–
172 56].

173 We used introduced range monk parakeet populations in the United States (U.S.) as
174 independent replicates of populations established following social disruption. Recent work
175 with monk parakeets supports the idea that the introduction process, including transport out of
176 the native range and housing in long-term captivity, represents a form of extreme social
177 disruption. Under naturalistic conditions, removing even a single individual from an
178 established social group consistently disrupts monk parakeets’ dominance ranks [53]. In the
179 U.S. introduced range, social disruption through the pet trade has occurred over short
180 evolutionary timescales, beginning about 50 years ago. The earliest sightings of monk

181 parakeets in the U.S. were reported in 1969, although populations in some states may have
182 been established in the 1980's or later [46,48]. In our previous work, we used the term
183 "invasive" to refer to monk parakeet populations outside of the native range [35,56]. We now
184 use the more inclusive term "introduced" to refer to these populations [57].

185 We used contact call recordings to infer which type of identity information was most
186 salient in learned monk parakeet vocal signals. We used this approach on both native and
187 introduced range contact calls to test whether the type of identity information was the same or
188 differed between the native and introduced ranges. Previous work demonstrated that the
189 strongest acoustic convergence in monk parakeet contact calls occurs at the individual scale
190 for native range populations in Uruguay (e.g. strong individual signatures) [35]. In addition,
191 acoustic structures that encoded individual vocal signatures in contact calls of introduced
192 range populations in the U.S. were simpler compared to native range contact calls in
193 Uruguay, which may be associated with signaling and learning in smaller local populations
194 compared to the native range [56]. This work in the introduced range did not assess the
195 relative strength of information encoding at the individual level compared to the group level in
196 contact calls. Whether simpler individual vocal signatures reflect an overall change in the type
197 of identity information encoded in contact calls after population disruption remains unknown,
198 and requires a combined approach to assess convergence at both of the individual and group
199 levels in the native and introduced ranges. We expected that if introduced populations had
200 recovered following social disruption, then the type of identity information in introduced range
201 contact calls would not change, such that both native and introduced populations would
202 exhibit the strongest acoustic convergence at the individual scale. However, if the introduction
203 process was sufficiently disruptive, then we expected that contemporary introduced range
204 parakeets would diverge from the type of identity information used in the native range, and
205 would instead display stronger acoustic convergence at a higher social scale. We placed our

206 results in the context of longer timescales by comparing against another parrot species with
207 strong contact call convergence at higher social scales and distinctive vocal dialects. Our
208 integration of quantitative approaches with a conceptual framework of hierarchical mapping
209 patterns can be used to evaluate stable identity information encoding in learned
210 communication signals more broadly across taxa. Together, our rigorous computational and
211 comparative approaches provide new insight into how identity information in learned vocal
212 signals can be robust to social disruption over ecological timescales, and can differ between
213 species representing longer evolutionary timescales.

214

215 **2. Methods**

216

217 *2.1 Ethics statement*

218 This research was conducted under an approved Institutional Animal Care and Use protocol
219 (IACUC no. 2017-006, New Mexico State University, USA) and an animal care and use
220 protocol approved by la Comisión de Ética en el Uso de Animales (CEUA no. 240011-002512-
221 17, la Universidad de la República, Uruguay).

222

223 *2.2 Recording contact calls*

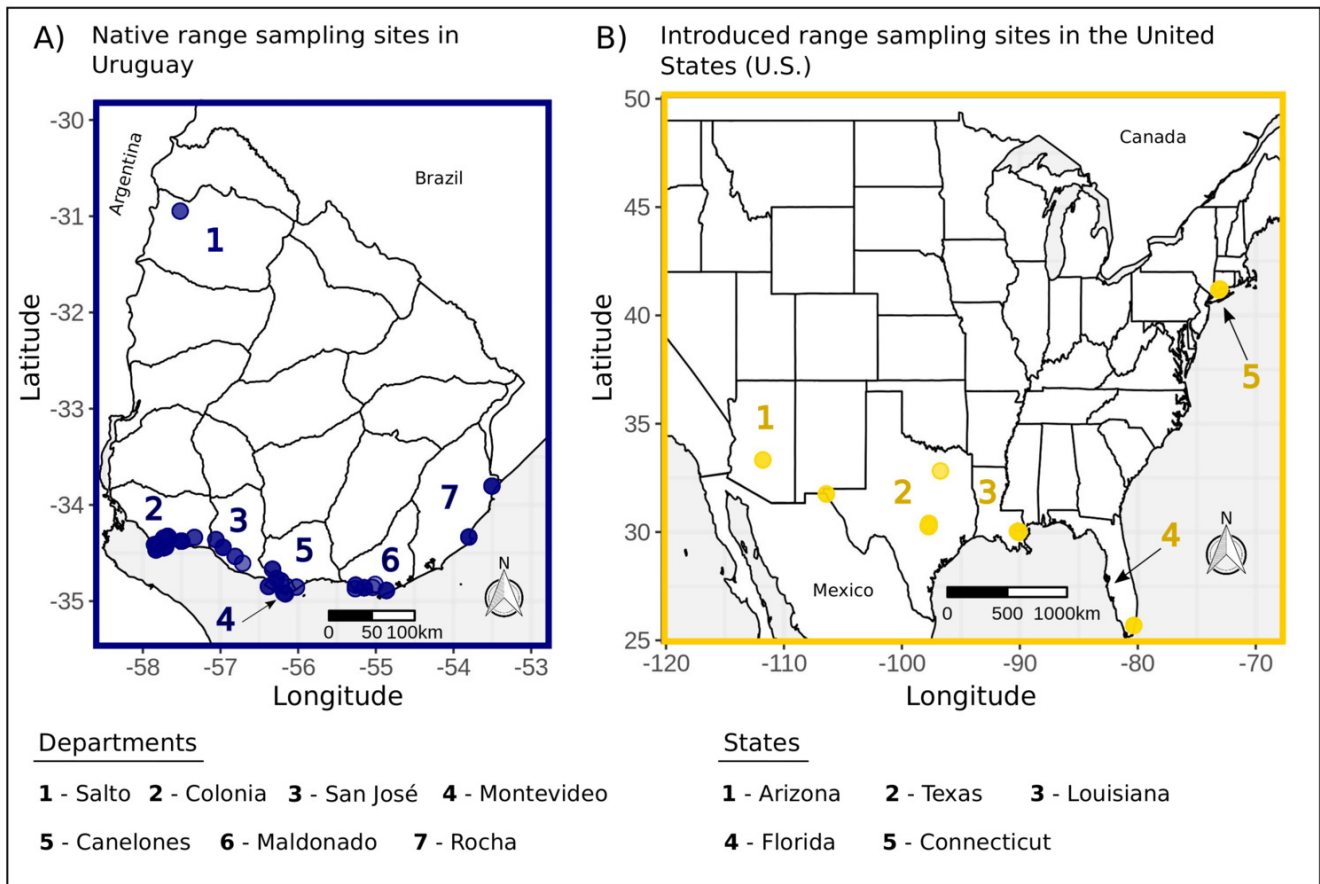
224 We recorded contact calls from native range monk parakeets in 2017 at 37 sites across 7
225 departments in Uruguay in our previous work [35]. Our introduced range dataset included
226 contact calls recorded at 26 sites across 5 states in the U.S. in 4 different sampling years:
227 2004, 2011, 2018, and 2019. In 2004, introduced range contact calls were recorded in
228 Connecticut, Florida, Louisiana, and Texas (calls were provided by the authors of [58]). We
229 recorded parakeets in Texas and Louisiana in 2011, Arizona in 2018, and Texas again in
230 2019. For our temporal analyses below, we relied on contact calls that we recorded in Texas

231 in 2004, 2011, and 2019 (3 sampling years), and contact calls recorded in Louisiana in 2004
232 and 2011 (2 sampling years, see S1 Appendix section 1).

233 Recording sessions in 2004 used Marantz PMD670 or PMD690 recorders with
234 Sennheiser ME67K6 shotgun microphones, and these recordings were digitized at 48000 Hz
235 and 16 bit depth [58]. In all other recording sessions we used Marantz PMD661 MKII and
236 PMD660 solid state recorders, Sennheiser ME67 long shotgun microphones and foam
237 windscreens, and we digitized our recordings at 44100 Hz sampling rate and 16 bit depth
238 [35,56]. All recorded individuals were unmarked, with the exception of a few marked
239 individuals in the native range [35].

240

241 **Fig 1. A map of contact call recording sites for native range populations in Uruguay**
 242 **and introduced range populations in the United States (U.S.).**
 243 We recorded parakeets across A) 7 departments in Uruguay and B) 5 states in the U.S. Our
 244 geographic sampling was more contiguous in the native range, which reflected the natural
 245 contiguity of populations across the southeastern coast of Uruguay, compared to the more
 246 geographically isolated populations in the U.S. introduced range. We used GADM shapefiles
 247 for the national and county borders of Uruguay (https://gadm.org/download_country.html).
 248 For the U.S., the country and state borders were originally sourced from Natural Earth
 249 (<https://www.naturalearthdata.com/>) and U.S. Census datasets
 250 ([https://www.census.gov/geographies/mapping-files/time-series/geo/cartographic-](https://www.census.gov/geographies/mapping-files/time-series/geo/cartographic-boundary.html)
 251 [boundary.html](https://www.census.gov/geographies/mapping-files/time-series/geo/cartographic-boundary.html)), respectively.
 252



253 *2.3 Pre-processing contact calls*

254 We manually selected contact calls from our field recordings. For our introduced range
255 recording sessions in later years, we selected contact calls using Raven version 1.4 [59],
256 consistent with native range contact call selection in [35]. The previously published introduced
257 range contact calls from 2004 were provided as clips of original recordings [58]. We
258 performed pre-processing for all introduced range contact calls, including the 2004 clips, with
259 the warbleR package [60] to implement the same quality control pipeline we had previously
260 used for native range contact calls (S1 Appendix section 1, [35,56]). Our quality control
261 criteria included contact calls with signal to noise ratios of 7 or higher (e.g. calls that were at
262 least 7 times louder than background noise) that also did not display loud signals or other
263 background noise that overlapped with contact call structure. We performed the majority of
264 our pre-processing and downstream analyses in the R software environment [61], including
265 the tidyverse [62].

266

267 *2.4 Social scales represented in our contact call datasets*

268 We obtained contact calls at two different social scales for the purposes of this study: the
269 individual scale, and a group scale that represented a higher level of social organization. To
270 assess contact call convergence at the individual scale, we repeatedly sampled known
271 individuals to obtain multiple exemplar contact calls produced by the same individual. This
272 individual-level dataset included 229 total contact calls from 8 native range birds (3 marked, 5
273 unmarked) recorded at 3 different sites in 2017, and 9 introduced range birds (all unmarked)
274 recorded at 7 different sites in either 2004, 2011, or 2019 (see Table A5 in [56]). Each
275 individual was recorded at one site only, and because the birds we recorded were generally
276 unmarked, we recorded repeat contact calls from particular individuals while the calling bird
277 was producing multiple contact calls within a short period of time (e.g. a few minutes [35]).

278 After pre-processing contact calls, our individual scale dataset included a median of 10
279 (range: 4 - 25) contact calls for the native range individuals and a median of 12 (range: 5 - 28)
280 contact calls for the introduced range individuals. Our individual scale dataset provided us
281 with sufficient sampling depth per individual to assess acoustic convergence at the individual
282 scale. We used this contact call dataset to represent individual vocal signatures over a short
283 sampling period for each repeatedly sampled individual. In previous work with this same
284 dataset, we identified individual vocal signatures encoded in frequency modulation patterns
285 [56], which are widely considered to be acoustic structures that animals can modify by
286 learning to create individually distinctive signals [24,26,63,64]. While individuals' physiological
287 states could influence subtle patterns of variation in learned vocalizations [65], studies with
288 other vocal learning taxa, such as bottlenose dolphins, have also identified individual vocal
289 signatures encoded in the frequency contours of learned vocalizations recorded over short
290 timescales [27,37].

291 To address contact call convergence at a group scale, we recorded and compared
292 contact calls across nesting sites. We used nesting sites as groups because parakeets likely
293 interact often with other individuals at the same nesting site. Monk parakeet nesting sites
294 include clusters of single or multi-chambered stick nests that are often built in close proximity
295 [66], and parakeets from nearby clusters of nests engage in social interactions [51], making it
296 difficult to determine the boundaries of independent nesting sites. In this study, we recorded at
297 clusters of nests that were geographically separate (the shortest distance among these
298 nesting sites was 0.15 km), which we refer to hereafter as "sites". For our site scale dataset,
299 we obtained a single contact call per bird at each site. Because the parakeets usually
300 produced only a single contact call when leaving or returning to their nests, we were limited to
301 sampling a single contact call per unmarked individual at this higher social scale.

302 After pre-processing, our site scale dataset included 1353 total contact calls recorded
303 at 63 sites (37 native range sites and 26 introduced range sites). Some introduced range sites
304 were repeatedly sampled in different sampling years (see Tables A3 and A4 in [56]). This
305 dataset contained a median of 15 (range: 5 - 53) and 15.5 (range: 5 - 91) contact calls across
306 the native and introduced range sites, respectively. Since we recorded a single contact call
307 per unique individual at each site, our site scale dataset did not provide sufficient resolution of
308 individual vocal signatures. However, this dataset allowed us to compare patterns of acoustic
309 variation at a higher scale of social organization over broader geographic areas in each range
310 (Fig 1).

311 To compare hierarchical mapping patterns between the native and introduced ranges,
312 we used 37 native range sites separated by 0.15 – 513.59 km across 7 departments in
313 Uruguay, and 18 introduced range sites across 5 U.S. states that were separated by 0.74 –
314 3502.98 km [35,56]. In our analyses below, we randomly selected a subsample of sites and
315 contact calls per site for calculations of acoustic convergence, and we repeated this process
316 over many resampling iterations, which allowed us to control for non-independence among
317 sites (e.g. sites separated by short geographic distances that may be easily traversed by
318 volant animals). To compare hierarchical mapping patterns over time in the introduced range,
319 we used a subsample of sites in Texas and Louisiana that were recorded in more than one
320 sampling year (see the respective number of sites and geographic distances in S1 Appendix
321 section 1). For our analyses at the site scale, we also generated 3 versions of the site scale
322 dataset to account for the possibility that some contact calls could represent repeated
323 sampling of the same unmarked individual(s) (S1 Appendix section 2). These 3 datasets
324 included the full dataset of contact calls, as well as the full dataset filtered by either clustering
325 with Gaussian mixture models in the mclust R package [67] or visual classification methods
326 with a custom-designed RShiny app [68] to remove contact calls that were likely to represent

327 such repeated individual sampling (S1 Appendix sections 3 - 7). Following contact call
328 similarity measurements, we performed analyses with these 3 site scale datasets to compare
329 the degree of repeated individual sampling in each of the native and introduced ranges, as
330 well as to assess the robustness of our overall results at this higher social scale. We used
331 separate contact call datasets at the individual and site scales under the assumption that our
332 sampling approach captured stable patterns of acoustic convergence, rather than the rapid
333 vocal matching that some parrots exhibit in real time [36,38,39]. In other words, if individuals
334 were using learning to stably converge on vocalizations at a given social scale, then we
335 expected to find relatively higher convergence at one social scale compared to the other,
336 regardless of the individuals that we sampled at each social scale.

337
338 *2.5 Measuring contact call similarity with spectrographic cross-correlation*

339 We used contact call similarity measurements to quantify hierarchical mapping patterns
340 across different social scales. For instance, if individuals were converging on shared contact
341 calls within sites, then we expected that contact calls compared within the same site would
342 exhibit high similarity measurements, and lower similarity measurements when compared to
343 contact calls from different sites. We measured contact call similarity with spectrographic
344 cross-correlation (SPCC) [69], which has traditionally been used in studies reporting patterns
345 of acoustic variation consistent with social learning of vocalizations in parrots
346 [23,24,30,31,35,36,38,58,70-73]. We performed SPCC with a Hanning window, a window
347 length of 378 samples, and a window overlap of 90 samples for Fourier transformations, as
348 well as Pearson's correlation method and a bandpass filter of 0.5 to 9kHz [60]. Unless
349 otherwise specified, we used these same parameters for subsequent spectrum-based
350 analyses. We conducted SPCC with all contact calls across the native and introduced ranges.

352 *2.6 Measuring contact call similarity with supervised machine learning*

353 We also measured similarity among monk parakeet contact calls using a supervised machine
354 learning approach that identifies biologically relevant patterns of variation in avian acoustic
355 signals [35,74,75]. As in our previous work [35], measuring similarity with a traditional method
356 (SPCC) and a newer method (supervised random forests), allowed us to verify that the
357 hierarchical mapping patterns we identified were not an artifact of using a single similarity
358 method. We built supervised random forests models with 1844 acoustic and image features,
359 including features derived from spectrographic cross-correlation (SPCC) and dynamic time
360 warping similarity measurements, standard spectral acoustic measurements, descriptive
361 statistics of Mel-frequency cepstral coefficients, and spectrogram image measurements (S1
362 Appendix sections 8 – 9). We used the warbleR and dtw R packages for acoustic
363 measurements [60,76], the software WNDCHRM for image measurements [77], and the
364 MASS and base R packages to extract features [61,78]. We trained random forests models to
365 classify contact calls back to 4 repeatedly sampled individuals in each of the native and
366 introduced ranges with the caret package (156 contact calls and 8 individuals total, S1
367 Appendix sections 10 – 11) [79,80]. We built and trained models on known repeatedly
368 sampled individuals because native range monk parakeet contact calls group visibly by
369 individual in a low dimensional trait space (e.g. two-dimensional acoustic space, S1 Fig) [35].
370 It is important to train classification models on discrete categories or classes [81], as a means
371 of ensuring that classification outcomes reflect biologically relevant variation, rather than
372 issues with how the models were built.

373 We built our first model with the full set of 1844 acoustic and image features. We built a
374 second model by performing automated feature selection and using the most important
375 features from that analysis (S1 Appendix section 11). Our second model outperformed the
376 first model, so we used the second model with 114 features for final analyses. To predict the

377 similarity of the individual scale contact calls that we used for validation, as well as the site
378 scale contact calls, we ran the remaining individual scale contact calls (73 total contact calls,
379 4 and 5 repeatedly sampled native and introduced range individuals, respectively) and the
380 1353 site scale contact calls down the final model. We extracted the resulting proximity matrix
381 as the random forests similarity measurements [35,74,75,82,83]. We performed our random
382 forests analyses with the caret, ranger, Boruta, and edarf R packages [80,84–86]. To validate
383 model performance, we used these similarity measurements to cluster the validation contact
384 calls with Gaussian mixture modeling in the R package mclust [67], which allowed us to
385 determine whether the random forests model identified biologically relevant patterns of
386 acoustic variation within and among contact calls of new individuals (e.g. individuals that were
387 not present in the training dataset).

388 After confirming that the final model captured relevant patterns of variation among the
389 individuals that we used to validate model performance, we used random forests similarity
390 measurements to generate low-dimensional acoustic space visualizations. Since we had used
391 the individual scale contact calls to train and validate the random forests model that we used
392 to predict contact call similarity, we did not use random forests similarity measurements to
393 perform quantitative analyses of acoustic convergence at the individual scale. Instead, we
394 used the training classification performance of our final random forests model, and the
395 clustering performance during validation with random forests similarity, to support our
396 individual scale analyses with SPCC similarity. Using two similarity methods to quantify
397 acoustic convergence at the site scale allowed us to validate that our results at this social
398 scale reflected biologically relevant variation, and did not arise from relying on a single
399 similarity method.

400

401 *2.7 Comparing native and introduced range hierarchical mapping patterns in acoustic space*

402 To assess hierarchical mapping patterns in each of the native and introduced ranges, we
403 compared patterns of acoustic convergence in low-dimensional acoustic space at the
404 individual and site social scales. To generate acoustic space for each similarity method, we
405 optimized non-metric multidimensional scaling (MDS) to reduce the dimensionality of the
406 SPCC and random forests similarity matrices, respectively, with the MASS R package [78]
407 (S1 Appendix section 12). For acoustic space at the individual scale, we used random forests
408 similarity obtained during model validation for 4 native range parakeets recorded at 3 sites in
409 the department of Colonia, Uruguay in 2017, and 4 introduced range birds recorded at 3 sites
410 in Austin, Texas, U.S. in 2019. For the site scale, we used both random forests and SPCC
411 similarity measurements for 4 native range sites in the department of Colonia, Uruguay in
412 2017, and 4 introduced range sites in Austin, Texas, U. S. in 2019. We also filtered the
413 acoustic space MDS coordinates by contact calls in each of the 3 site scale datasets that we
414 used to address repeated sampling of individuals (see section 2.4). Acoustic space can be
415 interpreted on the same axes for each similarity method but not compared between similarity
416 methods (e.g. acoustic space is different between SPCC and random forests analyses). We
417 interpreted contact calls that grouped together in acoustic space by individual or site as
418 structurally similar calls (e.g. high convergence), while calls dispersed in acoustic space were
419 structurally different (e.g. low convergence). We compared hierarchical mapping patterns
420 between the native and introduced ranges by comparing the relative patterns of overlap in
421 acoustic space among individuals or sites.

422

423 *2.8 Using Earth Mover's Distance to compare hierarchical mapping patterns between ranges*

424 Mantel tests have traditionally been used to correlate matrices of acoustic similarity with
425 matrices of binary categorical identity (e.g. individual or group identity) over many
426 permutations, in order to address whether vocalizations compared within categories are more

427 similar than vocalizations among categories (S1 Appendix sections 15 – 16), while also
428 controlling for non-independent data in pairwise symmetric matrices [23,35]. Due to recent
429 criticism of using Mantel tests to quantify acoustic convergence [54], we instead used Earth
430 Mover's Distance, or the minimum amount of work needed to convert one distribution into
431 another [87] to estimate the strength of acoustic convergence across social scales. Earth
432 Mover's Distance provides a conceptually similar approach to Mantel tests that can be used
433 to quantify and compare acoustic convergence. We compared hierarchical mapping patterns
434 between the native and introduced range populations by comparing the relative magnitude of
435 Earth Mover's Distance values at each social scale between ranges.

436 For this analysis, we obtained similarity values representing comparisons of contact
437 calls within and among categories at each social scale (e.g. comparisons of the same or
438 different individuals at the individual scale). We used the emdist R package [88] to calculate
439 Earth Mover's Distance as the minimum amount of work needed to convert distributions of the
440 same-category contact call comparisons into distributions of different-category contact call
441 comparisons. We performed these calculations in a single dimension bounded between 0 and
442 1 (e.g. the minimum and maximum possible similarity values). In these calculations, larger
443 values of Earth Mover's Distance are equivalent to stronger acoustic convergence. For
444 instance, if stronger convergence occurred at the individual scale, then similarity values for
445 contact calls compared for the same individual should be distributed closer to 1, while
446 similarity values for contact calls compared among individuals should be distributed closer to
447 0, and it should take more work, or greater Earth Mover's Distance, to convert one distribution
448 into the other. We calculated Earth Mover's Distance in a histogram-based approach with a
449 customized resampling routine to generate even sample sizes for calculations across social
450 scales. Our resampling routine also allowed us to control for variation in same-site

451 membership at the individual scale, as well as possible non-independence among sites at the
452 site scale (S1 Appendix section 13).

453

454 *2.9 Evaluating hierarchical mapping patterns over time in the introduced range*

455 We compared the relative magnitudes of Earth Mover's Distance calculations over time in two
456 U.S. cities to determine whether the strength of acoustic convergence at the site scale
457 changed over time in the introduced range. For these analyses, we used introduced range
458 populations that we had repeatedly recorded in Austin, Texas and New Orleans, Louisiana.
459 We calculated Earth Mover's Distance with the emdist package [88] with our customized
460 resampling routine for each year that we had sampled contact calls in each city, because we
461 did not always sample the same sites in each year. For Austin, we obtained Earth Mover's
462 Distance using different sites recorded in each of 3 sampling years: 3 sites in 2004, 5 sites in
463 2011, and 6 sites in 2019. For New Orleans, we calculated Earth Mover's Distance using
464 different sites sampled in 2 years: 3 sites in 2004 and 2 sites in 2011. We obtained Earth
465 Mover's Distance with random forests and SPCC similarity measurements, as well as each of
466 the 3 site scale datasets (the number of sites used in each city and year was smaller for the
467 datasets filtered after clustering and visual classification, S1 Appendix section 13). These
468 analyses were similar to those that we performed above to compare hierarchical mapping
469 patterns between ranges (section 2.8, S1 Appendix section 13). We also performed Mantel
470 test results over time in these introduced range cities (S1 Appendix section 17). Finally, we
471 addressed the possibility of population recovery since introduction by using the auk R
472 package [89] to evaluate population trends from eBird checklists in each city over our
473 sampling years (S1 Appendix section 14) [90].

474

475 *2.10 Comparing hierarchical mapping patterns with another parrot species*

476 We placed our results in a broader context by quantifying and directly comparing hierarchical
477 mapping patterns of native and introduced range monk parakeets with the yellow-naped
478 amazon, a species well-known for having regional group identity information in their contact
479 calls. These amazon parrots imitate the contact calls of conspecifics and exhibit distinctive
480 regional vocal dialects that are audibly perceptible to humans [23]. Such vocal sharing may
481 facilitate recognizing familiar group members [12,23]. Regional dialects in yellow-naped
482 amazon contact calls have provided a baseline for identifying strong acoustic convergence
483 within social groups for other vocal learning species [58,70,72], including monk parakeets
484 [35]. Here we used yellow-naped amazon contact calls as a point of reference for strong
485 acoustic convergence that could occur at a higher social scale in introduced range monk
486 parakeet contact calls if group membership information became more important to signal after
487 introduction than individual identity.

488 For our comparative analyses, we quantified hierarchical mapping patterns over the
489 individual and site social scales for native and introduced range monk parakeets (separately),
490 and over the individual, site, and regional dialect social scales for yellow-naped amazons.
491 For yellow-naped amazons, we used previously published contact calls recorded in Costa
492 Rica in 1994 [23]. We measured contact call similarity for each species using SPCC [60], and
493 selected similarity values for a subsample of individuals or groups at each social scale that
494 represented similar sampling depth and geographic breadth for each range and species (S1
495 Appendix sections 19 – 20). We compared hierarchical mapping patterns by assessing
496 patterns of relative overlap among distributions of the subsampled SPCC similarity values
497 within and among categories (e.g. individuals or groups).

498 We also designed a customized bootstrapping approach to quantify the strength of
499 acoustic convergence at each social scale for native range monk parakeets, invasive range
500 monk parakeets, and yellow-naped amazons that complemented and validated our analyses

501 with Earth Mover's Distance. In this analysis, we randomly selected 5 SPCC similarity values
502 within the given category and 5 SPCC similarity values among the given category in each
503 bootstrapping iteration (S1 Appendix section 21). This random sampling was performed with
504 replacement, such that SPCC values within or among categories could be randomly selected
505 more than once in the same iteration. We calculated bootstrapped similarity ratios by dividing
506 similarity values within the given category by similarity values among the given category. We
507 performed bootstrapping over 200 iterations and calculated 1000 total similarity ratios for
508 exemplars of each category (individual or group) at each social scale for native range
509 parakeets, introduced range parakeets, and yellow-naped amazons. Similarity ratios close to
510 1 pointed to weaker convergence. We used similarity ratios increasingly greater than 1 as
511 evidence of stronger convergence (e.g. contact calls were more similar within categories than
512 among categories).

513

514 **3. Results**

515 *3.1 Strong individual signatures in native and introduced range contact calls*

516 We identified strong acoustic convergence at the individual scale in contact calls recorded in
517 both ranges. Contact call lexicons (or collections of spectrograms) for known repeatedly
518 sampled individuals indicated that parakeets in each of the native and introduced ranges
519 consistently produced contact calls that were distinctive from those of other birds (Fig 2A).
520 This result was further supported by the general patterns of low overlap among individuals
521 that we identified in random forests and SPCC acoustic space, although there was higher
522 overlap among introduced range individuals (Figs 2B and S1).

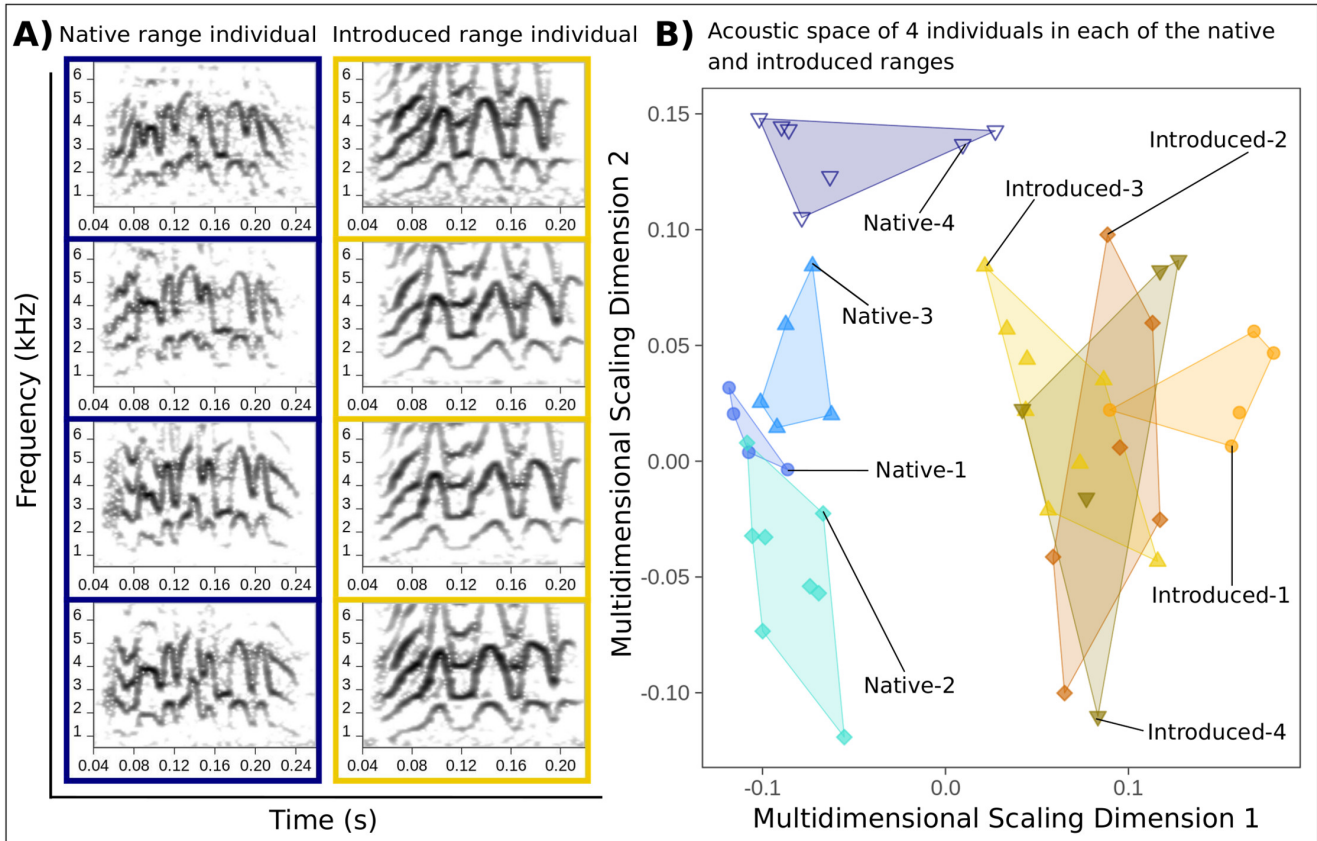
523 Our supervised machine learning results also pointed to strong acoustic convergence
524 at the individual scale. The final random forests model that we used for prediction displayed
525 high classification accuracy during training. The model classified contact calls back to the

526 individuals that we used for training with 97.44% accuracy (95% CI: 93.57 – 99.30%). The
527 mean \pm SE balanced accuracy of our model's classification performance per individual
528 (representing the averaged sensitivity and specificity) was similarly high for the 4 native range
529 (99.00% \pm 1%) and 4 introduced range training individuals (98.75% \pm 0.75%). Finally, our
530 analyses of the strength of acoustic convergence at the individual scale with Earth Mover's
531 Distance also supported strong individual signatures in native and introduced range contact
532 calls. The Earth Mover's Distance values that we calculated at the individual scale in each of
533 the native and introduced ranges were of similar magnitude (Native range mean and 95% CI:
534 0.159 (0.153, 0.164); Introduced range mean and 95% CI: 0.131 (0.125, 0.138), Table B in S1
535 Appendix). We obtained qualitatively similar results using Mantel tests (S1 Appendix section
536 16, Table D in S1 Appendix).

537

538 **Fig 2. Native and introduced range monk parakeets displayed strong individual vocal**
539 **signatures.**

540 In A) we show a lexicon with 4 contact calls for one repeatedly sampled bird in each of the
541 native and introduced ranges. In B), random forests acoustic space is shown for 4 native
542 range and 4 introduced range individuals. Each point represents a different contact call per
543 individual, and individual identities are encoded by shapes and hues. The convex hull
544 polygons demonstrate the area per individual in acoustic space. The blue palette corresponds
545 to the native range and gold-brown to the introduced range. See Table A in S1 Appendix for
546 decoded individual identities. Individuals generally produced visibly consistent contact calls
547 (A) that were also distinctive from other individuals (B).



549 *3.2 Contact call convergence within sites was low*

550 We found that individuals at the same site did not produce similar contact calls (Fig 3A).

551 When we assessed hierarchical mapping patterns in acoustic space, we found that contact

552 calls did not group by site identity. Instead, contact calls from the same site were

553 overdispersed, resulting in substantial overlap among different sites in acoustic space

554 generated using random forests similarity (Fig 3B), as well as SPCC similarity (S2 Fig). The

555 low degree of acoustic convergence that we identified at the site scale was supported by

556 Earth Mover's Distance values that were an order magnitude lower for the site scale

557 compared to the individual scale in each of the native and introduced ranges (Fig 4 and Table

558 B in S1 Appendix). This result held across the complementary SPCC and random forests

559 similarity methods that we used for Earth Mover's Distance calculations at the site scale (Fig

560 4).

561 We compared our Earth Mover's Distance results across the 3 site scale datasets to

562 determine how keeping or filtering out contact calls of potentially repeatedly sampled

563 individuals affected our results at this social scale. While the Earth Mover's Distance statistics

564 for the 3 native range site scale datasets were consistently low, values for the introduced

565 range varied more across the site scale datasets. The introduced range Earth Mover's

566 Distance values for each site scale dataset were uniformly greater than those we obtained for

567 the native range datasets using each similarity method (Table B in S1 Appendix). However,

568 despite this variation that we observed between ranges, and across site scale datasets for the

569 introduced range, all Earth Mover's Distance values at the site scale remained an order of

570 magnitude lower than the values we calculated at the individual scale in each of the native

571 and introduced ranges (Fig 4 and Table B in S1 Appendix). The highest Earth Mover's

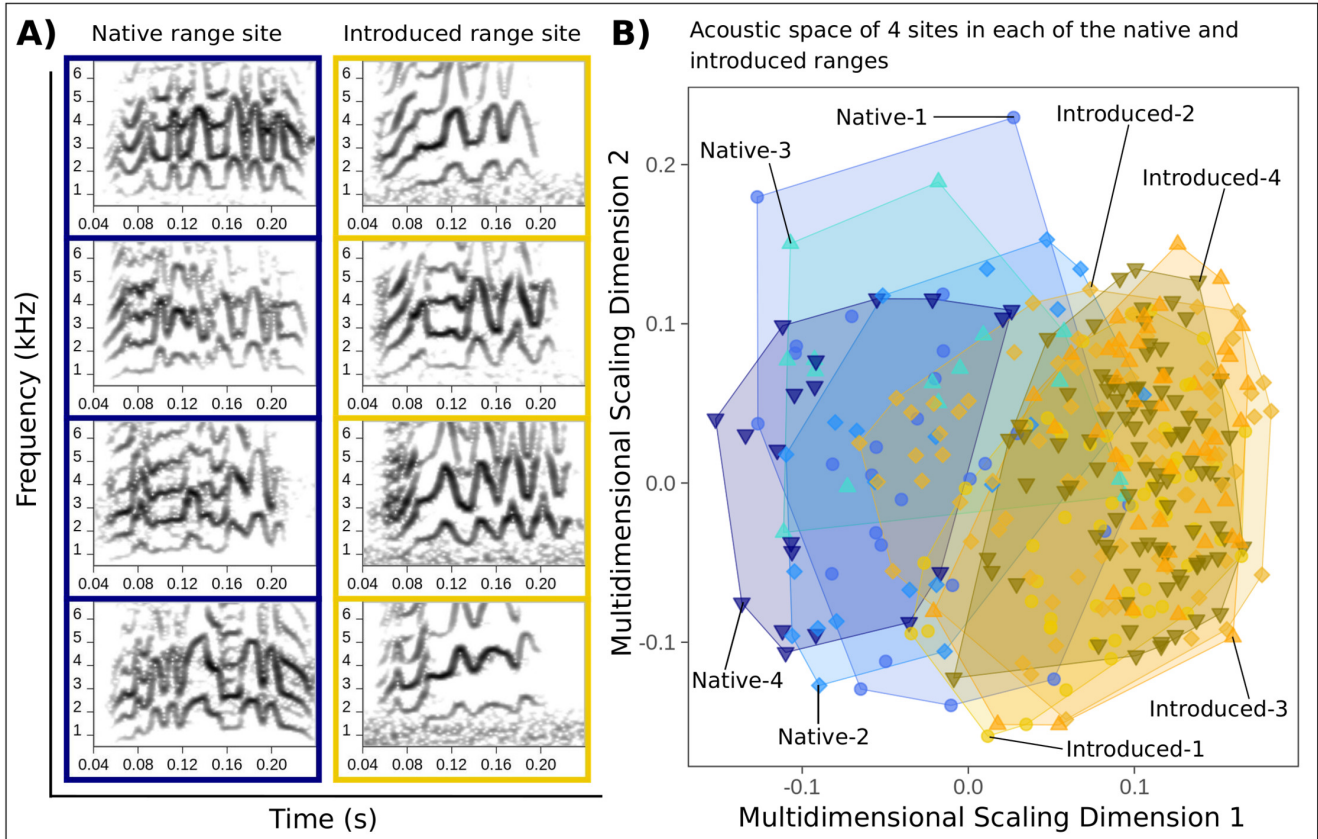
572 Distance values that we observed at the site scale for the native and introduced ranges

573 occurred with the full dataset of contact calls, in which we did not filter out contact calls

574 attributed to repeatedly sampled unmarked individuals at this social scale (Fig 4 and Table B
575 in S1 Appendix). We obtained similar results using Mantel tests (Table D in S1 Appendix).

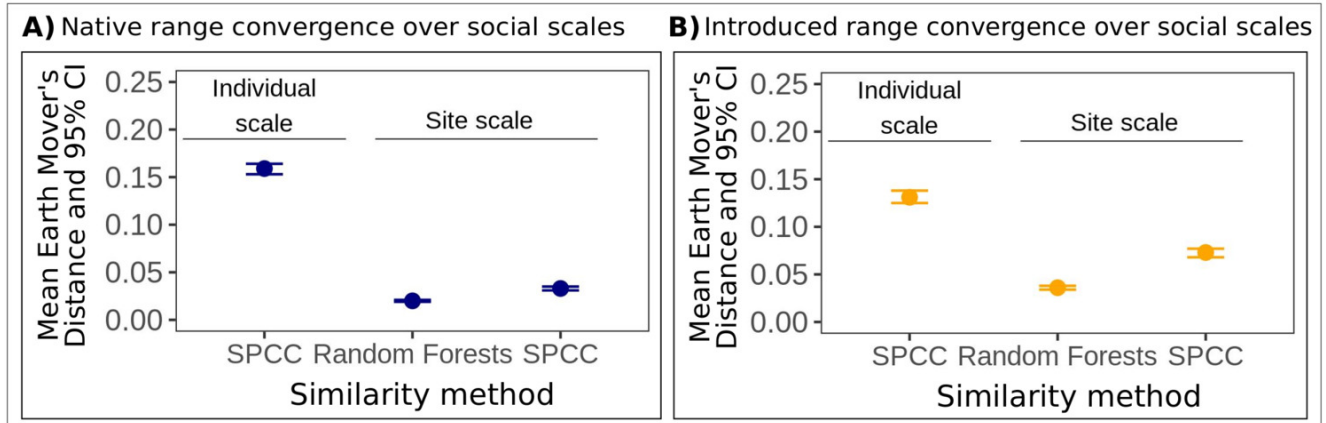
576 **Fig 3. We identified minimal acoustic convergence at the site scale in the native and**
577 **introduced ranges.**

578 In A) we show a lexicon of 4 contact calls each for one native range site and one introduced
579 range site, in which each contact call represents a unique individual. B) is a plot of random
580 forests acoustic space for 4 native range and 4 introduced range sites. The full dataset of
581 contact calls was used per site (see S2 Fig for the other site scale datasets). Across panels,
582 the color palettes, aesthetics, and polygons used are similar to Fig 2, but here encode site
583 identities. See Table A in S1 Appendix for decoded site identities. Contact calls within sites
584 were visibly different (A), and there was low differentiation among sites in acoustic space (B)
585 compared to the individual scale (Fig 2B).



587 **Fig 4. Acoustic convergence was stronger at the individual scale for native and**
588 **introduced range monk parakeets.**

589 We show Earth Mover's Distance measurements for A) native range monk parakeets, and B)
590 introduced range monk parakeets. In each panel, the symbols and error bars show the mean
591 individual and site scale Earth Mover's Distance values and 95% confidence intervals
592 calculated with spectrographic cross-correlation (SPCC) or random forests similarity. Higher
593 Earth Mover's Distance values indicate higher convergence, and we identified higher
594 convergence at the individual scale than at the site scale in both the native and introduced
595 ranges. The site scale values were calculated with the full contact call dataset at this social
596 scale.

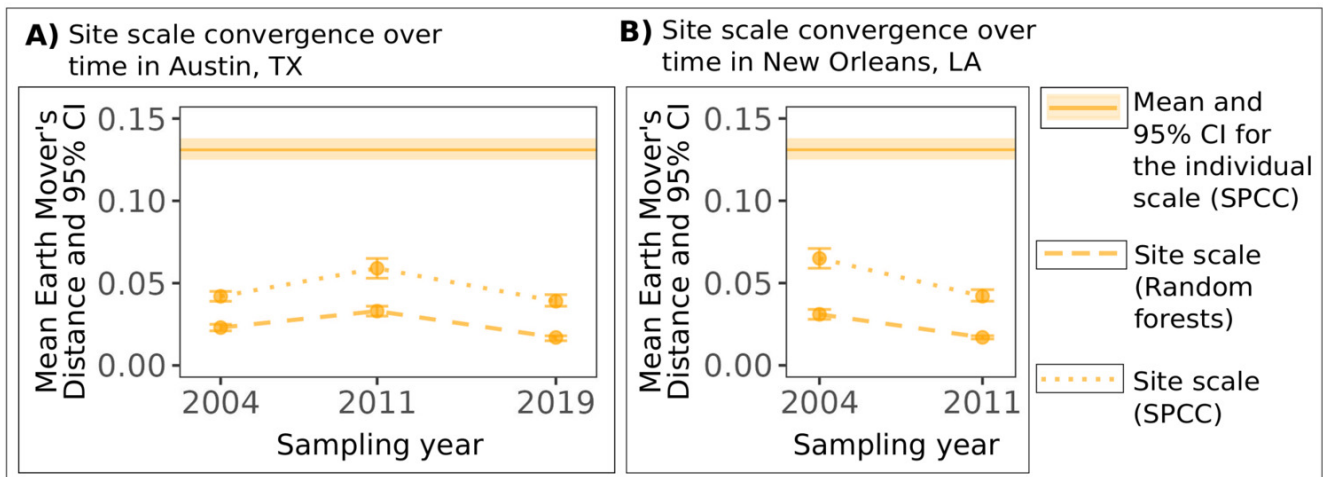


598 *3.3 Patterns of site scale convergence in the introduced range were consistent over time*

599 We did not identify clear evidence of temporal change in the strength of site scale acoustic
600 convergence in the introduced range (Fig 5 and Table C in S1 Appendix). In the city of Austin,
601 we identified higher Earth Mover's Distance values (indicating higher convergence) in 2011
602 using the all 3 site scale datasets for both SPCC and random forests similarity (Table C in S1
603 Appendix). For the city of New Orleans, we found the highest Earth Mover's Distance values
604 in 2004 using the full and visual classification datasets and both similarity methods (Table C in
605 S1 Appendix). Despite this variation, the Earth Mover's Distance values never reached the
606 same magnitude as convergence at the individual scale (Fig 5), but rather remained at the
607 same order of magnitude over time in each city (Table C in S1 Appendix). These Earth
608 Mover's Distance values that we calculated over time in each city were similar to the site-level
609 calculations that we obtained in our comparison between ranges (Tables B and C in S1
610 Appendix), and we found similar results using Mantel tests (Table E in S1 Appendix). We used
611 eBird checklists from these cities in an analysis of population trends over time, to address the
612 possibility that population size could have increased since establishment. However, we found
613 that the mean annual frequency of monk parakeets reported in complete checklists in Austin
614 and New Orleans remained low (less than 5% of all species sightings) and was also generally
615 consistent from 2004 to 2020 (S1 Appendix section 14 and S7 Fig).

616

617 **Fig 5. Introduced range acoustic convergence at the site scale remained low in two**
 618 **cities sampled over time**
 619 We show Earth Mover's Distance measurements for A) 3 sampling years in Austin, TX and B)
 620 2 sampling years in New Orleans, LA. The mean Earth Mover's Distance value calculated for
 621 the individual scale with SPCC similarity is shown as a point of reference (a solid horizontal
 622 line in each panel). The shading around the individual scale line represents the 95%
 623 confidence interval. Lower Earth Mover's Distance values indicate lower convergence, and
 624 site scale convergence over time in each city remained lower than individual scale
 625 convergence for the introduced range. In each panel, the symbols and error bars show the
 626 mean site scale Earth Mover's Distance values and 95% confidence intervals calculated with
 627 random forests (dashed lines) or spectrographic cross-correlation (SPCC) similarity (dotted
 628 lines). The site scale values were calculated with the full contact call dataset at this social
 629 scale.



631 *3.4 More repeated sampling of individuals in our introduced range site scale dataset*

632 Using clustering with Gaussian mixture models, and visual classification across multiple
633 observers, we attributed more contact calls in our introduced range site scale datasets to the
634 inadvertent repeated sampling of unmarked individuals compared to our native range site
635 scale datasets. The mean number of repeated individuals that we identified by our clustering
636 and visual classification filtering approaches were only slightly higher for the introduced range
637 than the native range (Table 1). However, we found that the mean number of contact calls
638 attributed to repeated individuals was nearly twofold greater for introduced range sites by
639 each of the clustering and visual classification approaches that we had used to identify
640 repeated sampling of individuals in our site scale datasets (Table 1).

641

642 **Table 1. Assessing the degree of repeated sampling of individuals at the site scale in**
 643 **each of the native and introduced ranges**
 644

Filtering approach	Range	Repeated individuals (mean \pm SE) ^a	Contact calls per repeated individual (mean \pm SE) ^b
Clustering	Native	3.14 \pm 0.37	10.0 \pm 1.60
	Introduced	3.23 \pm 0.51	18.0 \pm 4.75
Visual classification	Native	3.48 \pm 0.39	2.83 \pm 0.15
	Introduced	3.57 \pm 0.54	5.31 \pm 0.64

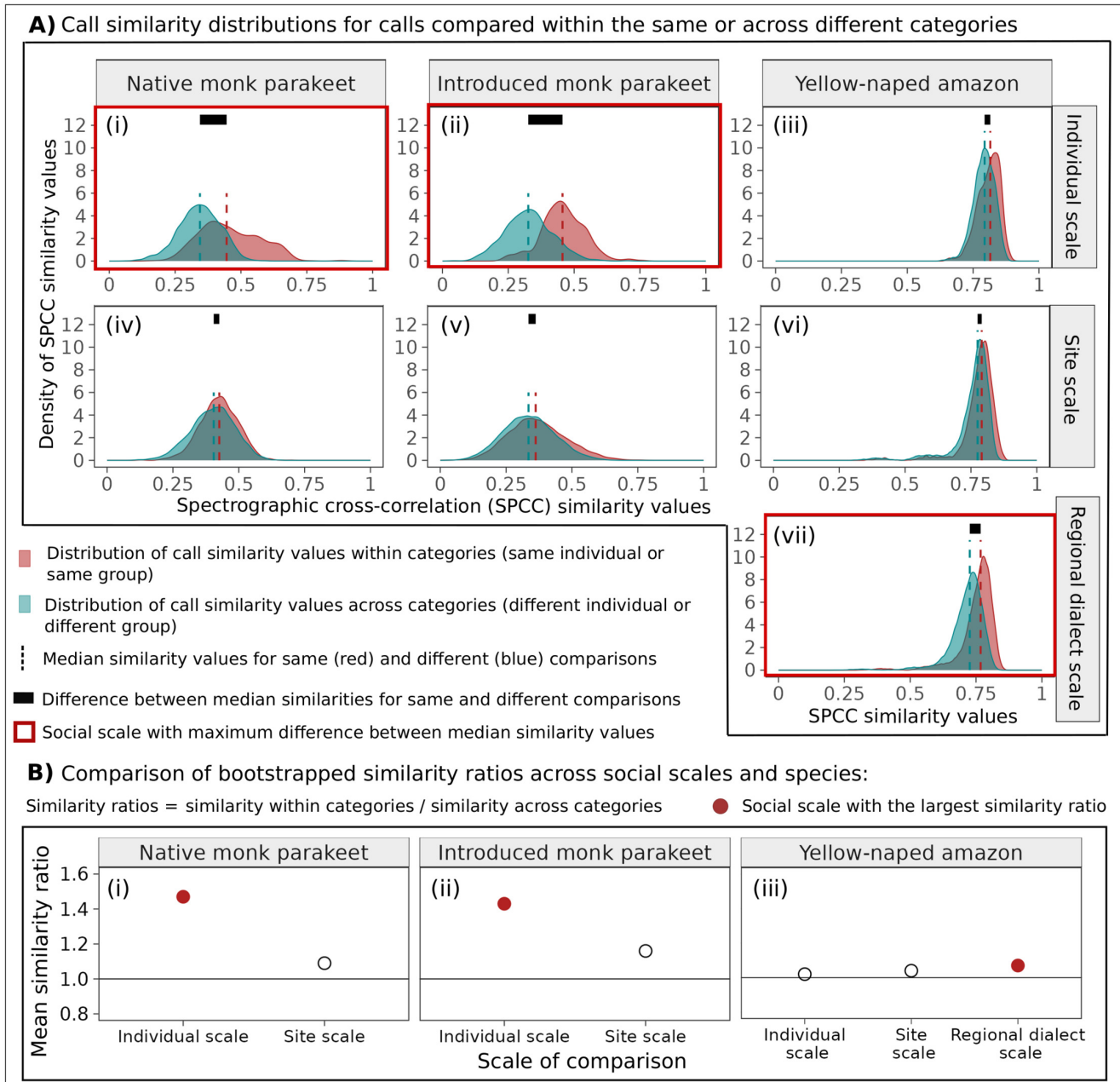
645 ^{a,b}These statistics were calculated with 36 native range and 22 introduced range sites,
 646 respectively, after removing 4 sites used for multi-observer reliability of visual classification
 647 (S1 Appendix section 6).

648 *3.5 Distinct hierarchical mapping patterns between monk parakeets and yellow-naped*
649 *amazons*

650 The hierarchical mapping patterns that we identified for both native and introduced range
651 monk parakeet contact calls differed from the hierarchical mapping patterns that we
652 recapitulated in yellow-naped amazon contact calls. Our results from this comparative
653 analysis showed that the individual scale was the social scale with the strongest acoustic
654 convergence in native and introduced range monk parakeet contact calls, while the regional
655 dialect scale displayed the strongest convergence in yellow-naped amazon contact calls. We
656 found that the greatest separation between the median similarity values of the two categories
657 of comparison per social scale (e.g. same or different individual or group) occurred at the
658 individual scale for native and introduced range monk parakeets (Fig 6A, panels i and ii). For
659 yellow-naped amazons, we detected the greatest separation between categories at the
660 regional dialect scale (Fig 6A, panel vii). In addition, the bootstrapped similarity ratios that we
661 used to assess the strength of acoustic convergence were greatest at the individual scale for
662 monk parakeets in each of the native and introduced ranges (Fig 6B, panels i and ii). In
663 contrast, the largest similarity ratio for yellow-naped amazons occurred at the regional dialect
664 scale (Fig 6B, panel iii).

665

666 **Fig 6. We compared hierarchical mapping patterns among contact calls of native and**
 667 **introduced range monk parakeets as well as yellow-naped amazons**
 668 In A) we show density curves for the distributions of spectrographic cross-correlation (SPCC)
 669 similarity values that represent comparisons of contact calls within or among categories in red and
 670 blue shading, respectively. The dashed lines represent the median similarity values per
 671 distribution. In B) we show the mean similarity ratios calculated from bootstrapped SPCC
 672 values. The solid line at 1 represents no convergence within a given category. For both native
 673 and introduced range monk parakeets, we show site scale results obtained from the full
 674 dataset of contact calls. In both A) and B), the social scale at which the strongest
 675 convergence occurred is shown in red.



677 **4. Discussion**

678 We asked whether the type of identity information that is important to communicate in learned
679 acoustic signals changed in introduced populations established after social disruption that
680 occurred over ecological timescales. We inferred that individual identity remained the most
681 important type of identity information to communicate in learned monk parakeet vocalizations,
682 even in populations established after repeated introductions to new parts of the world. We
683 discuss this new insight into the robustness of identity information encoded in learned
684 communication signals, and point to possible directions for future work over ecological and
685 evolutionary timescales.

686

687 *4.1 Hierarchical mapping patterns were similar between native and introduced range monk*
688 *parakeet populations*

689 Monk parakeets in native range populations in Uruguay and introduced range populations in
690 the U.S. emphasized individual identity information in learned vocalizations. In each range,
691 the hierarchical mapping patterns that we quantified in contact calls showed the strongest
692 convergence at the individual scale and weaker convergence within sites. These results were
693 robust to the greater degree of repeated individual sampling that we identified in our
694 introduced range site scale dataset (Table 1 and S1 Appendix section 18). In addition, the low
695 convergence that we identified at the site scale in two cities sampled over time, which
696 represented independent introduction events, suggested that these hierarchical mapping
697 patterns were unlikely to have changed in the broader U.S. introduced range over the
698 timespan of this study. We also recapitulated the structural differences previously identified
699 between native and introduced range contact calls that reflected the simplification of individual
700 vocal signatures associated with smaller local populations in the U.S. (see the separation in
701 acoustic space among native and introduced range contact calls in Figs 2B and 3B) [56]. This

702 simplification of individual vocal signatures post-introduction may explain the patterns of
703 greater overlap that we identified among introduced individuals in acoustic space (Fig 2), as
704 well as lower acoustic convergence at the individual scale for the introduced range compared
705 to the native range using Earth Mover's Distance (Fig 4 and Table B in S1 Appendix).
706 However, despite these differences at the individual scale between ranges, we found that
707 acoustic convergence at the individual scale was consistently an order of magnitude greater
708 than convergence at the site scale in each of the native and introduced ranges. This overall
709 result of stronger convergence at the individual scale and weaker convergence at the site
710 scale in monk parakeet contact calls was supported by the two methods that we used to
711 measure call similarity (SPCC and random forests), as well as the two analytical approaches
712 that we used to quantify acoustic convergence (Earth Mover's Distance and a customized
713 bootstrapping routine). Using two methods to measure contact call similarity, as well as two
714 methods to quantify acoustic convergence, allowed us to validate the weaker convergence
715 that we identified at the site scale in each of the native and introduced ranges.

716 Our analyses indicate that individual identity remained the most important type of
717 identity information to communicate to receivers, even in introduced populations. In other
718 words, we inferred that the type of identity information emphasized in learned contact calls
719 was robust to social disruption that occurred over short evolutionary timescales (less than 50
720 years ago when monk parakeets were introduced to the U.S. [46,48]). Although some
721 features of the social environment changed after introduction, such as the smaller local
722 population sizes that we identified in previous work [56], monk parakeets' social environments
723 may have been generally robust to introduction or were re-established after initial
724 perturbations. If the individually distinctive contact calls that we identified in the native and
725 introduced ranges are used for individual vocal recognition, then parakeets in each range
726 should be engaging in social interactions that favor signaling individual identity in learned

727 communication signals, which is an idea that can be tested in future work. Our quantitative
728 approaches with vocal signals allowed us to reach this inference without depending on the
729 time- and resource-intensive collection of social data. These findings do not preclude the
730 possibility that social interactions at higher scales of social organization are important in this
731 species. While relationships at the pair level are important for monk parakeets, this species
732 consistently forms social groups with multiple levels of social organization in captive settings
733 [50–53,91].

734 Signaling individual identity information in learned vocalizations could instead reflect a
735 more fixed aspect of vocal communication systems, such as developmental constraints or
736 genetic encoding of receivers' perceptual abilities. Future work could also address the stability
737 of individual identity information encoding in learned contact calls across different social
738 contexts, given that some vocal learning species exhibit rapid convergence or divergence that
739 appears conditional on the social context [36–39], and in others, individual vocal signatures
740 [92] or individually-distinctive repertoires of shared contact calls appear to change over time
741 [93].

742

743 *4.2 Comparing our results against a parrot species that exhibits regional vocal dialects*

744 We performed a comparative analysis with yellow-naped amazon contact calls to place our
745 ecological comparison of native and introduced range monk parakeet contact calls in an
746 evolutionary context. If introduced range monk parakeets switched to emphasizing group
747 membership information in contact calls, then hierarchical mapping patterns in introduced
748 range monk parakeet contact calls should have exhibited stronger convergence at a higher
749 social scale. We used yellow-naped amazons as a baseline for comparison because this
750 species exhibits strong acoustic convergence at a higher social scale with regional vocal
751 dialects that are audibly and visibly distinctive to humans [23,30,31,94]. We found that

752 hierarchical mapping patterns were similar between native and introduced range monk
753 parakeets, supporting our conclusion that identity information in monk parakeet contact calls
754 did not change after social disruption that occurred over ecological timescales. In this
755 comparative analysis, we used a customizing bootstrapping approach that yielded similar
756 results for native range and introduced range monk parakeets as our analyses with Earth
757 Mover's Distance and Mantel tests.

758 Our comparative analysis also highlighted the importance of using quantitative tools to
759 complement human perception of audible and visible variation in avian vocalizations. When
760 relying on the human ear and eye, the variation among regional dialects in yellow-naped
761 amazon contact calls is far more perceptible than individually distinctive monk parakeet
762 contact calls. For example, the regional dialects that we recapitulated in the amazon contact
763 calls are distinctive to the human ear [23], including North dialect contact calls that sound like
764 "wah-wah", and variants of the South dialect that sound like "weeup". In contrast, patterns of
765 individual variation in monk parakeet contact calls are difficult to distinguish by the human ear,
766 and contact calls of different individuals all sound like "chees". However, when we used
767 quantitative methods to compare hierarchical mapping patterns between species, we found
768 that individual scale convergence in native and introduced range monk parakeet contact calls
769 was stronger than regional dialect convergence for yellow-naped amazons (Fig 6A: panels i,
770 ii, and vii).

771 Amazon vocal dialects may be more perceptible to humans than monk parakeet
772 individual vocal signatures because of humans' limited abilities to perceive fine-scale temporal
773 variation at higher frequencies [95,96]. Parrots' auditory perception abilities appear tuned for
774 higher frequencies, such as orange-fronted conures (*Eupsittula canicularis*), which display the
775 greatest auditory sensitivity in a frequency band that overlaps with the greatest spectral
776 energies in contact calls [97]. In addition, yellow-naped amazon contact calls exhibit slower

777 frequency modulation patterns that are more perceptible to humans, and can also be
778 arranged into fewer categories (e.g. a few regional dialects), a task that should pose reduced
779 cognitive challenges compared to categorizing monk parakeet contact calls by many different
780 individuals [1,98]. Overall, our results from this comparative analysis point to the importance
781 of using computational approaches to identify information in animal signals that is difficult for
782 humans to perceive but may be critical in animal communication systems.

783

784 *4.3 Future research considerations with hierarchical mapping patterns*

785 We combined computational tools with a conceptual framework of how hierarchical mapping
786 patterns are connected to identity signaling in animal vocal signals. This combined approach
787 allowed us to quantify hierarchical mapping patterns and then infer the most salient identity
788 information encoded in vocal signals. Similar computational approaches could be applied to
789 quantify hierarchical mapping patterns with existing datasets of animal signals to learn more
790 about the social environments in which individuals communicate across a broader range of
791 taxa, without depending on the time-intensive collection of social data from marked
792 individuals. When communication signals are learned, hierarchical mapping patterns should
793 capture overall patterns of acoustic variation that represent both active convergence or
794 divergence within social groups, as well as the side-effects of learning from others in a given
795 social group (e.g. vocalizations can be similar when individuals learned from templates that
796 happened to be similar). Here, we used the social scale with the strongest acoustic
797 convergence to infer which type of identity information animals are actively encoding in
798 learned vocalizations (e.g. the type of identity information that is most important to
799 communicate). In our conceptual framework, we considered stronger acoustic convergence
800 as active convergence, and weaker patterns of acoustic convergence as stochastic outcomes
801 associated with learning. For instance, monk parakeet contact calls recorded at the same site

802 did display a degree of convergence (Table B in S1 Appendix), albeit minimal, which should
803 be expected when animals are learning to sound different from others and are learning from
804 the same social group or set of templates.

805 Whether and how animals perceive and use stronger or weaker patterns of acoustic
806 convergence in learned vocalizations can be assessed experimentally using playbacks of
807 contact call variants. Indeed, the hierarchical mapping patterns identified for a particular
808 population or species can be used as an important foundation for designing biologically
809 relevant playback experiments, which can be more time-consuming than recording
810 communication signals, and are fundamental to understanding how receivers use the
811 information that signalers communicate. Playback experiments are important because
812 mismatches can occur between the social information encoded in signals and the information
813 that receivers use for social recognition, especially when it is cognitively costly to track certain
814 types of information [3,99]. Addressing how different types of identity information are used by
815 receivers will be important, since distantly related avian taxa, including vulturine guineafowl
816 (*Acryllium vulturinum*) and superb fairy-wrens (*Malurus cyaneus*), exhibit multilevel social
817 structures in the wild, suggesting that hierarchical social structures may be more
818 taxonomically widespread than traditionally thought [100,101].

819 While quantifying hierarchical mapping patterns can yield exciting insights into the
820 identity information that may be important to communicate, researchers should be careful
821 when using these patterns to inform new research directions about identity signaling and
822 social systems. Recording unmarked individuals in natural populations provides only a
823 snapshot of dynamic social interactions, as well as the social information conveyed in signals
824 that is important in a given social environment. For instance, sampling a few vocalizations per
825 individual over a short time frame makes it difficult to assess how identity information
826 encoding may change during dynamic social interactions, such as the rapid vocal matching

827 exhibited by wild orange-fronted conures and rose-breasted cockatoos (*Eolophus*
828 *roseicapillus*) [36,38,39]. In addition, while the literature has focused on social recognition in
829 more complex social environments with larger social groups and repeated interactions among
830 many individuals [6,12,28,29,99], future work could also address how learned identity signals
831 should change in social environments characterized by fewer individuals and differentiated
832 relationships overall.

833

834 **5. Conclusions**

835 We used native and introduced range monk parakeet contact calls to test whether the type of
836 identity information encoded in learned vocalizations changed in populations that were
837 established after social disruption that occurred over the last 50 years. We used
838 computational tools, including supervised machine learning, to quantify and compare
839 hierarchical mapping patterns in contact calls between the native and introduced ranges. We
840 inferred that identity information encoding was robust to social disruption over short ecological
841 timescales. By comparing hierarchical mapping patterns between monk parakeet and yellow-
842 naped amazon contact calls, we found that identity information encoding in learned parrot
843 vocalizations changed over longer evolutionary timescales. Our results suggest that signaling
844 systems facilitated by socially learned vocalizations can be robust to changes in social
845 conditions over short timescales, despite the flexibility generally attributed to socially learned
846 behaviors. Taken together, our findings point to exciting new research directions on the
847 flexibility or robustness of socially learned communication signals over short evolutionary
848 timescales.

849

850

851

852

853

854

855

856

857

858

859

860

861

862

863

864

865

866

867

868

869

870

871

872

873

874

875 **Acknowledgments:** We thank Clara Hansen and Tania Molina for help with fieldwork in
876 Uruguay. We also thank many others for their support throughout native range fieldwork as

877 acknowledged in [35], and are especially grateful to Dr. Enrique Lessa, Dr. Bettina Tassino,
878 Dr. Ivanna Tomasco, Gabino Suanes, Claudia Pérez, Patricia Vargas, Dr. Ethel Rodríguez
879 and Instituto Nacional de Investigación Agropecuaria (INIA) directors Dario Hirigoyen and
880 Santiago Cayota for their help coordinating fieldwork in Uruguay. We thank Dr. Kevin Burgio
881 for his support during crowdfunding with Experiment.com. We are grateful to Zoë Amerigian
882 and Alexandra Bicki for their help during fieldwork in the U.S. in 2019, and Dominique
883 Hellmich for her assistance with fieldwork in Arizona in 2018 and helping with visual
884 classification of contact calls. We are also grateful to Dr. Susannah Buhrman-Deever and Dr.
885 Jack Bradbury for providing monk parakeet contact calls recorded in 2004 and their
886 enthusiastic support of this research.

887

888 **References**

- 889 1. Bradbury JW, Vehrencamp SL. Principles of animal communication. 1st ed. Sunderland,
890 MA, USA: Sinauer Associates, Inc.; 1998.
- 891 2. Seyfarth RM, Cheney DL, Bergman T, Fischer J, Zuberbühler K, Hammerschmidt K.
892 The central importance of information in studies of animal communication. *Anim Behav.*
893 2010;80(1):3–8. doi: 10.1016/j.anbehav.2010.04.012
- 894 3. Bergman TJ. Experimental evidence for limited vocal recognition in a wild primate:
895 Implications for the social complexity hypothesis. *Proc R Soc B Biol Sci.*
896 2010;277(1696):3045–53. doi: 10.1098/rspb.2010.0580
- 897 4. Hobson EA. Differences in social information are critical to understanding aggressive
898 behavior in animal dominance hierarchies. *Curr Opin Psychol.* 2020;33:209–15. doi:
899 10.1016/j.copsyc.2019.09.010
- 900 5. Hobson EA, Mønster D, DeDeo S. Aggression heuristics underlie animal dominance
901 hierarchies and provide evidence of group-level social information. *Proc Natl Acad Sci*
902 *U S A.* 2021;118(10):e2022912118. doi: 10.1073/pnas.2022912118
- 903 6. Ramos-Fernandez G, King AJ, Beehner JC, Bergman TJ, Crofoot MC, Di Fiore A, et al.
904 Quantifying uncertainty due to fission–fusion dynamics as a component of social
905 complexity. *Proc R Soc B Biol Sci.* 2018;285(1879):20180532. doi:
906 10.1098/rspb.2018.0532

- 907 7. Furuyama T, Kobayasi KI, Riquimaroux H. Role of vocal tract characteristics in
908 individual discrimination by Japanese macaques (*Macaca fuscata*). *Sci Rep.*
909 2016;6(January):32042. doi: 10.1038/srep32042
- 910 8. Prior NH, Smith E, Lawson S, Ball GF, Dooling RJ. Acoustic fine structure may encode
911 biologically relevant information for zebra finches. *Sci Rep.* 2018;8(1):6212. doi:
912 10.1038/s41598-018-24307-0
- 913 9. Rendall D, Owren MJ, Rodman PS. The role of vocal tract filtering in identity cueing in
914 rhesus monkey (*Macaca mulatta*) vocalizations. *J Acoust Soc Am.* 1998;103(1):602–14.
915 doi: 10.1121/1.421104
- 916 10. Boughman JW, Wilkinson GS. Greater spear-nosed bats discriminate group mates by
917 vocalizations. *Anim Behav.* 1998;55(6):1717–32. doi: 10.1006/anbe.1997.0721
- 918 11. Nowicki S, Searcy WA. The evolution of vocal learning. *Curr Opin Neurobiol.*
919 2014;28:48–53. doi: 10.1016/j.conb.2014.06.007
- 920 12. Sewall KB, Young AM, Wright TF. Social calls provide novel insights into the evolution of
921 vocal learning. *Anim Behav.* 2016;120:163–72. doi: 10.1016/j.anbehav.2016.07.031
- 922 13. Janik VM, Slater PJB. Context-specific use suggests that bottlenose dolphin signature
923 whistles are cohesion calls. *Anim Behav.* 1998;56(4):829–38. doi:
924 10.1006/anbe.1998.0881
- 925 14. Jones BL, Daniels R, Tufano S, Ridgway S. Five members of a mixed-sex group of
926 bottlenose dolphins share a stereotyped whistle contour in addition to maintaining their
927 individually distinctive signature whistles. *PLoS One.* 2020;15(5):e0233658. doi:
928 10.1371/journal.pone.0233658
- 929 15. Nousek AE, Slater PJB, Wang C, Miller PJO. The influence of social affiliation on
930 individual vocal signatures of northern resident killer whales (*Orcinus orca*). *Biol Lett.*
931 2006;2(4):481–4. doi: 10.1098/rsbl.2006.0517
- 932 16. Rendell LE, Whitehead H. Vocal clans in sperm whales (*Physeter macrocephalus*).
933 *Proc R Soc B Biol Sci.* 2003;270(1512):225–31. doi: 10.1098/rspb.2002.2239
- 934 17. Watwood SL, Tyack PL, Wells RS. Whistle sharing in paired male bottlenose dolphins,
935 *Tursiops truncatus*. *Behav Ecol Sociobiol.* 2004;55(6):531–43. doi: 10.1007/s00265-
936 003-0724-y
- 937 18. Boughman JW. Vocal learning by greater spear-nosed bats. *Proc R Soc B Biol Sci.*
938 1998;265(1392):227–33. doi: 10.1098/rspb.1998.0286
- 939 19. Mammen DL, Nowicki S. Individual differences and within-flock convergence in
940 chickadee calls. *Behav Ecol Sociobiol.* 1981;9(3):179–86. doi: 10.1007/BF00302935

- 941 20. Sewall KB. Limited adult vocal learning maintains call dialects but permits pair-
942 distinctive calls in red crossbills. *Anim Behav.* 2009;77(5):1303–11. doi:
943 10.1016/j.anbehav.2009.01.033
- 944 21. Sewall KB. Early learning of discrete call variants in red crossbills: Implications for
945 reliable signaling. *Behav Ecol Sociobiol.* 2011;65(2):157–66. doi: 10.1007/s00265-010-
946 1022-0
- 947 22. Martinez TM, Logue DM. Conservation practices and the formation of vocal dialects in
948 the endangered Puerto Rican parrot, *Amazona vittata*. *Anim Behav.* 2020;166:261–71.
949 doi: 10.1016/j.anbehav.2020.06.004
- 950 23. Wright TF. Regional dialects in the contact call of a parrot. *Proc R Soc London, B.*
951 1996;263:867–72. doi: 10.1098/rspb.1996.0128
- 952 24. Berg KS, Delgado S, Okawa R, Beissinger SR, Bradbury JW. Contact calls are used for
953 individual mate recognition in free-ranging green-rumped parrotlets, *Forpus passerinus*.
954 *Anim Behav.* 2011;81(1):241–8. doi: 10.1016/j.anbehav.2010.10.012
- 955 25. Berg KS, Delgado S, Cortopassi KA, Beissinger SR, Bradbury JW. Vertical transmission
956 of learned signatures in a wild parrot. *Proc R Soc B Biol Sci.* 2012;279(1728):585–91.
957 doi: 10.1098/rspb.2011.0932
- 958 26. Janik VM, Sayigh LS, Wells RS. Signature whistle shape conveys identity information to
959 bottlenose dolphins. *Proc Natl Acad Sci U S A.* 2006;103(21):8293–7. doi:
960 10.1073/pnas.0509918103
- 961 27. Kershenbaum A, Sayigh LS, Janik VM. The encoding of individual identity in dolphin
962 signature whistles: how much information is needed? *PLoS One.* 2013;8(10):e77671.
963 doi: 10.1371/journal.pone.0077671
- 964 28. Pollard KA, Blumstein DT. Social group size predicts the evolution of individuality. *Curr*
965 *Biol.* 2011;21(5):413–7. doi: 10.1016/j.cub.2011.01.051
- 966 29. Tibbetts EA, Dale J. Individual recognition: It is good to be different. *Trends Ecol Evol.*
967 2007;22(10):529–37. doi: 10.1016/j.tree.2007.09.001
- 968 30. Salinas-Melgoza A, Wright TF. Evidence for vocal learning and limited dispersal as dual
969 mechanisms for dialect maintenance in a parrot. *PLoS One.* 2012;7(11):e48667. doi:
970 10.1371/journal.pone.0048667
- 971 31. Wright TF, Dahlin CR, Salinas-Melgoza A. Stability and change in vocal dialects of the
972 yellow-naped amazon. *Anim Behav.* 2008;76(3):1017–27. doi:
973 10.1016/j.anbehav.2008.03.025
- 974 32. Wright TF, Rodriguez AM, Fleischer RC. Vocal dialects, sex-biased dispersal, and
975 microsatellite population structure in the parrot *Amazona auropalliata*. *Mol Ecol.*
976 2005;14(4):1197–205. doi: 10.1111/j.l365-294X.2005.02466.x

- 977 33. Casey C, Reichmuth C, Costa DP, Le Boeuf B. The rise and fall of dialects in northern
978 elephant seals. *Proc R Soc B Biol Sci.* 2018;285(1892):20182176. doi:
979 10.1098/rspb.2018.2176
- 980 34. Barker AJ, Vevjurko G, Bennett NC, Hart DW, Mograby L, Lewin GR. Cultural
981 transmission of vocal dialect in the naked mole-rat. *Science.* 2021;371(6528):503–7.
982 doi: 10.1126/science.abc6588
- 983 35. Smith-Vidaurre G, Araya-Salas M, Wright TF. Individual signatures outweigh social
984 group identity in contact calls of a communally nesting parrot. *Behav Ecol.*
985 2020;31(2):448–58. doi: 10.1093/beheco/arz202
- 986 36. Balsby TJS, Bradbury JW. Vocal matching by orange-fronted conures (*Aratinga*
987 *canicularis*). *Behav Processes.* 2009;82(2):133–9. doi: 10.1016/j.beproc.2009.05.005
- 988 37. King SL, Janik VM. Bottlenose dolphins can use learned vocal labels to address each
989 other. *Proc Natl Acad Sci.* 2013;110(32):13216–21. doi: 10.1073/pnas.1304459110
- 990 38. Scarl JC, Bradbury JW. Rapid vocal convergence in an Australian cockatoo, the galah
991 *Eolophus roseicapillus*. *Anim Behav.* 2009;77(5):1019–26. doi:
992 10.1016/j.anbehav.2008.11.024
- 993 39. Vehrencamp SL, Ritter AF, Keever M, Bradbury JW. Responses to playback of local vs.
994 distant contact calls in the orange-fronted conure, *Aratinga canicularis*. *Ethology.*
995 2003;109(1):37–54. doi: 10.1046/j.1439-0310.2003.00850.x
- 996 40. Aplin LM. Culture and cultural evolution in birds: A review of the evidence. *Anim Behav.*
997 2019;147:179–87. doi: 10.1016/j.anbehav.2018.05.001
- 998 41. Dlugosch KM, Parker IM. Founding events in species invasions: Genetic variation,
999 adaptive evolution, and the role of multiple introductions. *Mol Ecol.* 2008;17(1):431–49.
1000 doi: 10.1111/j.1365-294X.2007.03538.x
- 1001 42. Blackburn TM, Pysek P, Bacher S, Carlton JT, Duncan RP, Jarosik V, et al. A proposed
1002 unified framework for biological invasions. *Trends Ecol Evol.* 2011;26(7):333–9. doi:
1003 10.1016/j.tree.2011.03.023
- 1004 43. Carrete M, Edelaar P, Blas J, Serrano D, Potti J, Dingemanse N, et al. Don't neglect
1005 pre-establishment individual selection in deliberate introductions. *Trends Ecol Evol.*
1006 2012;27(2):67–8.
- 1007 44. Chapple DG, Simmonds SM, Wong BBM. Can behavioral and personality traits
1008 influence the success of unintentional species introductions? *Trends Ecol Evol.*
1009 2012;27(1):57–64. doi: 10.1016/j.tree.2011.09.010
- 1010 45. Bradbury JW, Balsby TJS. The functions of vocal learning in parrots. *Behav Ecol*
1011 *Sociobiol.* 2016;70:293–312. doi: 10.1007/s00265-016-2068-4

- 1012 46. Edelaar P, Roques S, Hobson EA, Goncalves Da Silva A, Avery ML, Russello MA, et al.
1013 Shared genetic diversity across the global invasive range of the monk parakeet
1014 suggests a common restricted geographic origin and the possibility of convergent
1015 selection. *Mol Ecol.* 2015;24(9):2164–76. doi: 10.1111/mec.13157
- 1016 47. Hobson EA, Smith-Vidaurre G, Salinas-Melgoza A. History of nonnative monk
1017 parakeets in Mexico. *PLoS One.* 2017;12(9):e0184771. doi:
1018 10.1371/journal.pone.0184771
- 1019 48. Russello MA, Avery ML, Wright TF. Genetic evidence links invasive monk parakeet
1020 populations in the United States to the international pet trade. *BMC Evol Biol.*
1021 2008;8:217. doi: 10.1186/1471-2148-8-217
- 1022 49. Smith-Vidaurre G. Patterns of genetic and acoustic variation in a biological invader.
1023 New Mexico State University; 2020.
- 1024 50. Hobson EA, Avery ML, Wright TF. An analytical framework for quantifying and testing
1025 patterns of temporal dynamics in social networks dynamics in social networks. *Anim*
1026 *Behav.* 2013;85(1):83–96. doi: 10.1016/j.anbehav.2012.10.010
- 1027 51. Hobson EA, Avery ML, Wright TF. The socioecology of monk parakeets: insights into
1028 parrot social complexity. *Auk.* 2014;131:756–75. doi: 10.1642/AUK-14-14.1
- 1029 52. Hobson EA, John DJ, McIntosh TL, Avery ML, Wright TF. The effect of social context
1030 and social scale on the perception of relationships in monk parakeets. *Curr Zool.*
1031 2015;61(1):55–69. doi: 10.1093/czoolo/61.1.55
- 1032 53. van der Marel A, Francis X, O’Connell CL, Estien CO, Carminito C, Moore VD, et al.
1033 Perturbations highlight importance of social history in parakeet rank dynamics. *Behav*
1034 *Ecol.* 2023;34(3):457–67. doi: 10.1093/beheco/arad015
- 1035 54. Smeele SQ, Tyndel SA, Aplin LM, McElreath MB. Multi-level analysis of monk parakeet
1036 vocalisations shows emergent dialects between cities in the European invasive range.
1037 *bioRxiv.* 2022;1–17. doi: 10.1101/2022.10.12.511863
- 1038 55. Smeele SQ, Senar JC, Aplin LM, McElreath MB. Evidence for vocal signatures and
1039 voice-prints in a wild parrot. *bioRxiv.* 2023;1–18. doi: 10.1101/2023.01.20.524864
- 1040 56. Smith-Vidaurre G, Perez-Marrufo V, Wright TF. Individual vocal signatures show
1041 reduced complexity following invasion. *Anim Behav.* 2021;179:15–39. doi:
1042 10.1016/j.anbehav.2021.06.020
- 1043 57. Cheng SJ, Gaynor KM, Moore AC, Darragh K, Estien CO, Hammond JW, et al.
1044 Championing inclusive terminology in ecology and evolution. *Trends Ecol Evol.* 2023;1–
1045 4. doi: 10.1016/j.tree.2022.12.011

- 1046 58. Buhrman-Deever SC, Rappaport AR, Bradbury JW. Geographic variation in contact
1047 calls of feral North American populations of the monk parakeet. *Condor*.
1048 2007;109(2):389–98. doi: 10.1093/condor/109.2.389
- 1049 59. The Cornell Lab of Ornithology Bioacoustics Research Program. Raven Pro: Interactive
1050 sound analysis software. Ithaca, NY: The Cornell Lab of Ornithology; 2014.
- 1051 60. Araya-Salas M, Smith-Vidaurre G. warbleR: An R package to streamline analysis of
1052 animal acoustic signals. *Methods Ecol Evol*. 2017;8(2):184–91. doi: 10.1111/2041-
1053 210X.12624
- 1054 61. R Core Team. R: A language and environment for statistical computing. R Foundation
1055 for Statistical Computing, Vienna, Austria; 2022.
- 1056 62. Wickham H, Averick M, Bryan J, Chang W, McGowan LD, François R, et al. Welcome to
1057 the Tidyverse. *J Open Source Softw*. 2019;4(43):1686. doi: 10.21105/joss.01686
- 1058 63. Fripp D, Owen C, Quintana-Rizzo E, Shapiro A, Buckstaff K, Jankowski K, et al.
1059 Bottlenose dolphin (*Tursiops truncatus*) calves appear to model their signature whistles
1060 on the signature whistles of community members. *Anim Cogn*. 2005;8(1):17–26. doi:
1061 10.1007/s10071-004-0225-z
- 1062 64. Janik VM, Slater PJB. The different roles of social learning in vocal communication.
1063 *Anim Behav*. 2000;60(1):1–11. doi: 10.1006/anbe.2000.1410
- 1064 65. Janik VM, Knörnschild M. Vocal production learning in mammals revisited. *Philos Trans*
1065 *R Soc B Biol Sci*. 2021;376(1836):20200244. doi: 10.1098/rstb.2020.0244
- 1066 66. Eberhard JR. Breeding biology of the monk parakeet. *Wilson Bull*. 1998;110(4):463–73.
- 1067 67. Scrucca L, Fop M, Murphy TB, Raftery AE. mclust 5: Clustering, classification and
1068 density estimation using Gaussian finite mixture models. *R J*. 2016;8(1):289–317.
- 1069 68. Chang W, Cheng J, Allaire JJ, Xie Y, McPherson J. shiny: Web application framework
1070 for R. 2018.
- 1071 69. Clark CW, Marler P, Beeman K. Quantitative analysis of animal vocal phonology: An
1072 application to swamp sparrow song. *Ethology*. 1987;76:101–15. doi: 10.1111/j.1439-
1073 0310.1987.tb00676.x
- 1074 70. Bradbury JW, Cortopassi KA, Clemmons JR. Geographical variation in the contact calls
1075 of orange-fronted parakeets. *Auk*. 2001;118(4):958–72. doi: 10.1093/auk/118.4.958
- 1076 71. Eberhard JR, Zager I, Ferrer-Paris JR, Rodríguez-Clark K. Contact calls of island
1077 Brown-throated Parakeets exhibit both character and variance shifts compared to calls
1078 of their mainland relatives. *Ornithology*. 2022;139:1–18. doi:
1079 10.1093/ornithology/ukab076

- 1080 72. Guerra JE, Cruz-Nieto J, Ortiz-Maciel SG, Wright TF. Limited geographic variation in the
1081 vocalizations of the endangered thick-billed parrot: Implications for conservation
1082 strategies. *Condor*. 2008;110(4):639–47. doi: 10.1525/cond.2008.8609
- 1083 73. Salinas-Melgoza A, Renton K. Geographic variation in vocalisations of the Military
1084 Macaw in western Mexico. *Bioacoustics*. 2021;30(2):197–214. doi:
1085 10.1080/09524622.2020.1714479
- 1086 74. Humphries GRW, Buxton RT, Jones IL. Machine learning techniques for quantifying
1087 geographic variation in Leach's storm-petrel (*Hydrobates leucorhous*). In: Humphries
1088 GRW, Magness DR, Huettmann F, editors. *Machine Learning for Ecology and*
1089 *Sustainable Natural Resource Management*. Cham, Switzerland: Springer Nature;
1090 2018. p. 295–312. doi: 10.1007/978-3-319-96978-7_15
- 1091 75. Keen S, Ross JC, Griffiths ET, Lanzone M, Farnsworth A. A comparison of similarity-
1092 based approaches in the classification of flight calls of four species of North American
1093 wood-warblers (Parulidae). *Ecol Inform*. 2014;21:25–33. doi:
1094 10.1016/j.ecoinf.2014.01.001
- 1095 76. Giorgino T. Computing and visualizing dynamic time warping alignments in R: the dtw
1096 package. *J Stat Softw*. 2009;31(7):1–24. doi: 10.18637/jss.v031.i07
- 1097 77. Shamir L, Orlov N, Eckley DM, Macura T, Johnston J, Goldberg IG. Wndchrm - an open
1098 source utility for biological image analysis. *Source Code Biol Med*. 2008;3:1–13. doi:
1099 10.1186/1751-0473-3-13
- 1100 78. Venables WN, Ripley BD. *Modern Applied Statistics with S*. New York: Fourth Edition,
1101 Springer; 2002.
- 1102 79. Breiman L. Random forests. *Mach Learn*. 2001;45:5–32. doi:
1103 10.1023/A:1010933404324
- 1104 80. Kuhn M. Building predictive models in R using the caret package. *J Stat Softw*.
1105 2008;28(5):1–26. doi: 10.18637/jss.v028.i05
- 1106 81. Kuhn M, Johnson K. *Applied predictive modeling*. New York, New York, USA: Springer
1107 Science+Business Media; 2013.
- 1108 82. Keen SC, Odom KJ, Webster MS, Kohn GM, Wright TF, Araya-Salas M. A machine
1109 learning approach for classifying and quantifying acoustic diversity. *Methods Ecol Evol*.
1110 2021;12(7):1213–25. doi: 10.1111/2041-210x.13599
- 1111 83. Odom KJ, Araya-Salas M, Morano JL, Ligon RA, Leighton GM, Taff CC, et al.
1112 *Comparative bioacoustics: A roadmap for quantifying and comparing animal sounds*
1113 *across diverse taxa*. *Biol Rev*. 2021;96(4):1135–59. doi: 10.1111/brv.12695
- 1114 84. Jones ZM, Linder FJ. edarf: Exploratory data analysis using random forests. *J Open*
1115 *Source Softw*. 2016;1(6):92. doi: 10.21105/joss.00092

- 1116 85. Kursa MB, Rudnicki WR. Feature selection with the Boruta package. *J Stat Softw.* 2010;36(11):1–13. doi: 10.18637/jss.v036.i11
1117
- 1118 86. Wright MN, Ziegler A. ranger: A fast implementation of random forests for high
1119 dimensional data in C++ and R. *J Stat Softw.* 2017;77(1):1–17. doi:
1120 10.18637/jss.v077.i01
- 1121 87. Rubner Y, Tomasi C, Guibas LJ. The Earth Mover’s Distance as a metric for image
1122 retrieval. *Int J Comput Vis.* 2000;40(2):99.
- 1123 88. Urbanek S, Rubner Y. emdist: Earth Mover’s Distance. 2022.
- 1124 89. Strimas-Mackey M, Miller E, Hochachka W. auk: eBird data extraction and processing
1125 with AWK. R package version 0.4.1. 2018.
- 1126 90. Sullivan BL, Wood CL, Iff MJ, Bonney RE, Fink D, Kelling S. eBird: A citizen-based bird
1127 observation network in the biological sciences. *Biol Conserv.* 2009;142(10):2282–92.
1128 doi: 10.1016/j.biocon.2009.05.006
- 1129 91. van der Marel A, Prasher S, Carminito C, O’Connell CL, Phillips A, Kluever BM, et al. A
1130 framework to evaluate whether to pool or separate behaviors in a multilayer network.
1131 *Curr Zool.* 2021;67(1):101–11. doi: 10.1093/cz/zoaa077
- 1132 92. Zdenek CN, Heinsohn R, Langmore NE. Vocal individuality, but not stability, in wild palm
1133 cockatoos (*Probosciger aterrimus*). *Bioacoustics.* 2018;27(1):27–42. doi:
1134 10.1080/09524622.2016.1272004
- 1135 93. Dahlin CR, Young AM, Cordier B, Mundry R, Wright TF. A test of multiple hypotheses for
1136 the function of call sharing in female budgerigars, *Melopsittacus undulatus*. *Behav Ecol*
1137 *Sociobiol.* 2014;68(1):145–61. doi: 10.1007/s00265-013-1631-5
- 1138 94. Wright TF, Dahlin CR. Vocal dialects in parrots: patterns and processes of cultural
1139 evolution. *Emu - Austral Ornithol.* 2018;118(1):50–66. doi:
1140 10.1080/01584197.2017.1379356
- 1141 95. Dooling RJ, Leek MR, Gleich O, Dent ML. Auditory temporal resolution in birds:
1142 discrimination of harmonic complexes. *J Acoust Soc Am.* 2002;112(2):748–59. doi:
1143 10.1121/1.1494447
- 1144 96. Lohr B, Dooling RJ, Bartone S. The discrimination of temporal fine structure in call-like
1145 harmonic sounds by birds. *J Comp Psychol.* 2006;120(3):239–51. doi: 10.1037/0735-
1146 7036.120.3.239
- 1147 97. Wright TF, Cortopassi KA, Bradbury JW, Dooling RJ. Hearing and vocalizations in the
1148 orange-fronted conure (*Aratinga canicularis*). *J Comp Psychol.* 2003;117(1):87–95. doi:
1149 10.1037/0735-7036.117.1.87

- 1150 98. Wiley RH. Specificity and multiplicity in the recognition of individuals: Implications for
1151 the evolution of social behaviour. *Biol Rev.* 2013;88(1):179–95. doi: 10.1111/j.1469-
1152 185X.2012.00246.x
- 1153 99. Bergman TJ, Beehner JC. Measuring social complexity. *Anim Behav.* 2015;103:203–9.
1154 doi: 10.1016/j.anbehav.2015.02.018
- 1155 100. Camerlenghi E, McQueen A, Delhey K, Cook CN, Kingma SA, Farine DR, et al.
1156 Cooperative breeding and the emergence of multilevel societies in birds. *Ecol Lett.*
1157 2022;25(4):766–77. doi: 10.1111/ele.13950
- 1158 101. Papageorgiou D, Christensen C, Gall GEC, Klarevas-Irby JA, Nyaguthii B, Couzin ID,
1159 et al. The multilevel society of a small-brained bird. *Curr Biol.* 2019;29(21):R1120–1.
1160 doi: 10.1016/j.cub.2019.09.072
1161

1162 **Supporting Information:**

1163

1164 **S1 Appendix. Supplementary information about our sampling and analytical pipelines.**

1165 This document provides more details about the datasets that we used as well as each of our
1166 customized analytical pipelines with monk parakeet and yellow-naped amazon contact calls.

1167 This appendix also contains Tables A through E.

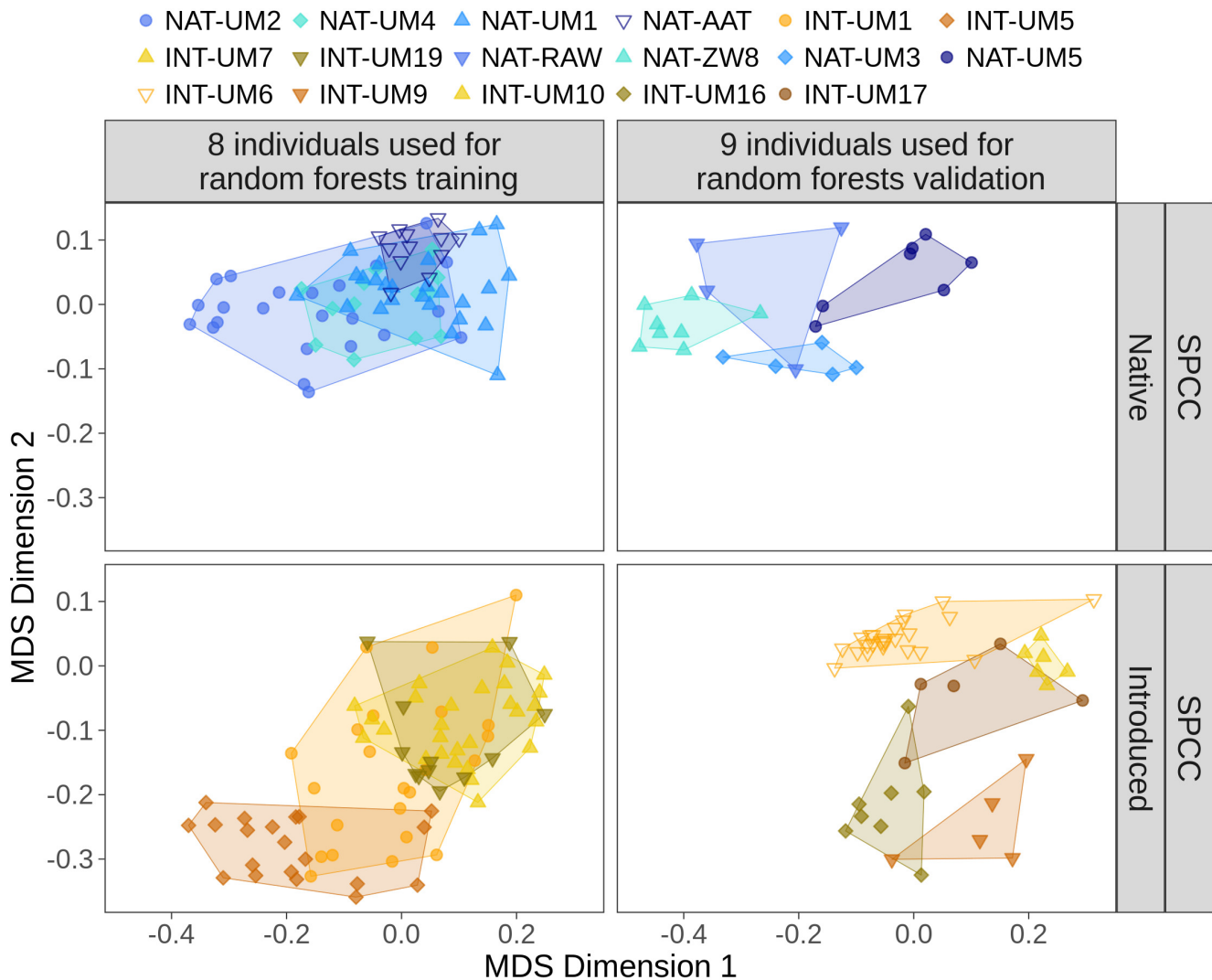
1168

1169 **S1 Fig. Similar patterns of acoustic convergence at the individual scale for native and**
1170 **introduced range monk parakeets using spectrographic cross-correlation (SPCC).**

1171 All 4 panels show SPCC acoustic space generated by multidimensional scaling (MDS) for
1172 contact calls of repeatedly sampled monk parakeets in each of the native and introduced
1173 ranges. Top left panel: 4 native range individuals that were used to train supervised random
1174 forests models. Bottom left panel: 4 introduced range individuals that we used to train
1175 supervised random forests models. Top right panel: 4 native range individuals were used to
1176 validate supervised random forests models. Bottom right panel: 5 introduced range individuals
1177 that were used to validate supervised random forests models. Blue palettes correspond to the
1178 native range and gold-brown palettes to the introduced range. In each panel, points represent

1179 different calls per repeatedly sampled individual. Individual identities are displayed through
 1180 shapes and hues per range, and convex hull polygons demonstrate the area encompassed
 1181 per individual in acoustic space. The acoustic space across all 4 panels can be interpreted on
 1182 the same axes. Here, individuals were overdispersed in acoustic space, pointing to strong
 1183 individual signatures in each range. These results were similar to our findings with random
 1184 forests similarity (Fig 2).

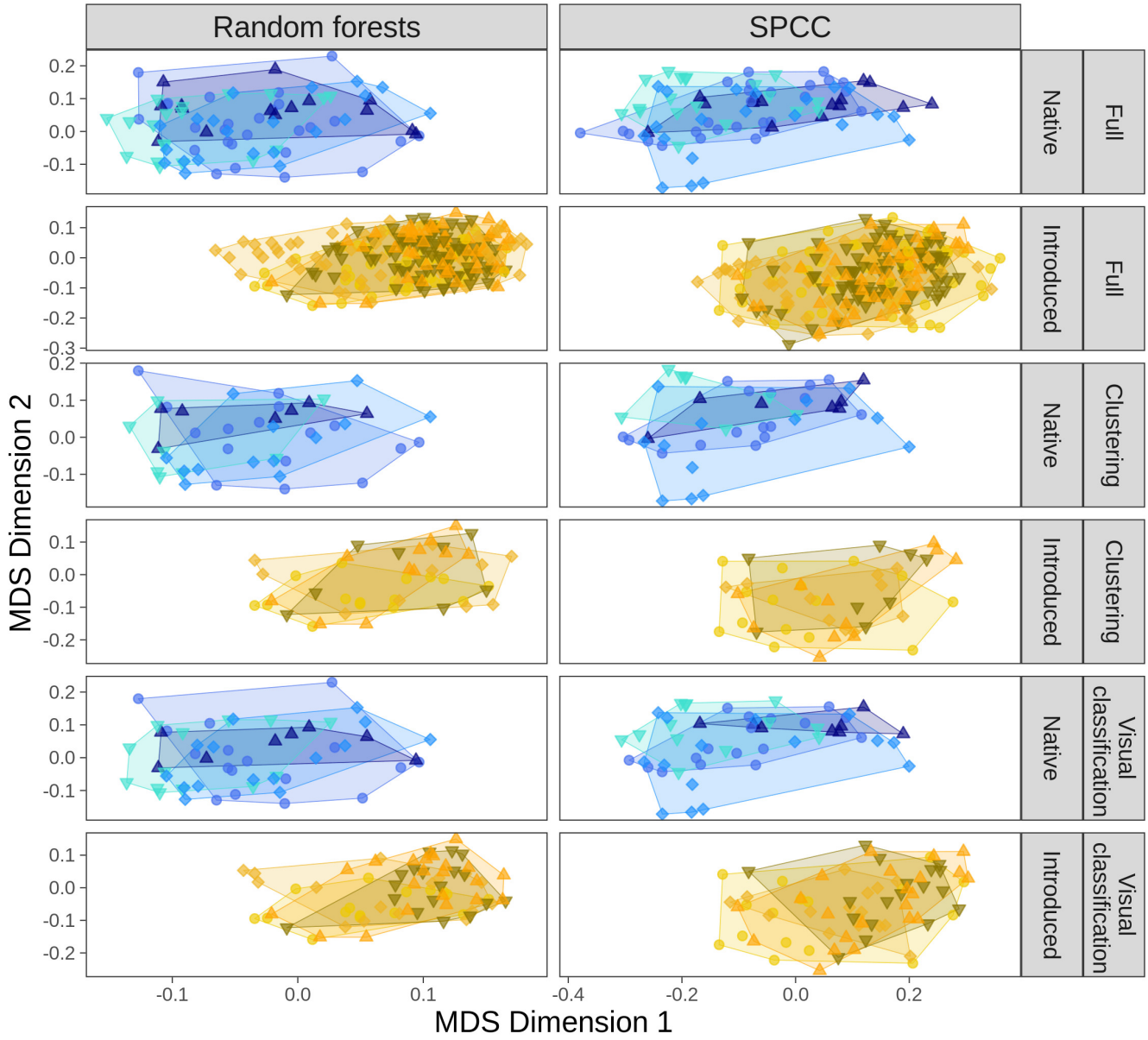
1185



1187

1188 **S2 Fig. Low acoustic convergence at the site scale in each range, as well as across the**
1189 **3 site scale datasets used to address potential repeated sampling of individuals.**
1190 Plots of random forests acoustic space are shown by similarity method (columns), as well as
1191 the three datasets used to address repeated individual sampling in each of the native and
1192 introduced ranges (rows). Acoustic space for the clustering and visual classification datasets
1193 were generated by filtering multidimensional scaling (MDS) coordinates for the full dataset of
1194 calls. The 4 sites shown here and the aesthetics used per range are the same as in Fig 3 in
1195 the main text.

● INES-08 ◆ PIED ▲ ROSA ▼ LENA ● ELEM ◆ INTR ▲ MART ▼ SOCC

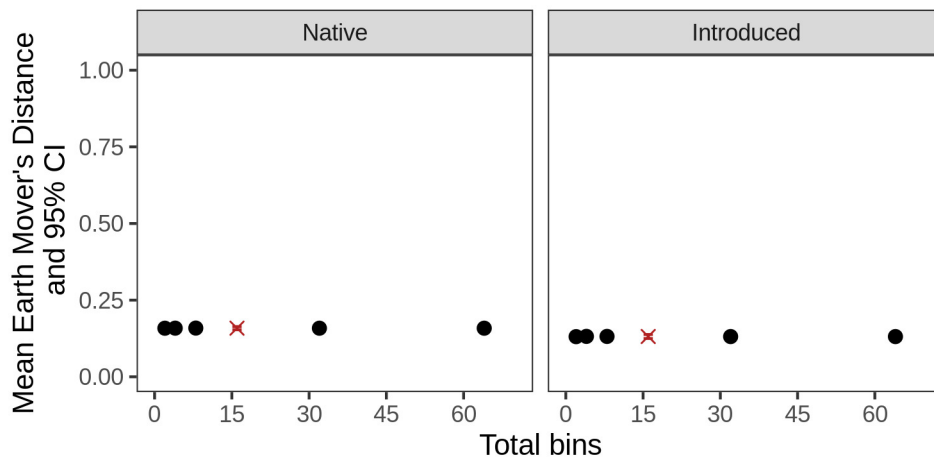


1197 **S3 Fig. Earth Mover's Distance individual scale results were consistent across total bin**
1198 **numbers in each of the native and introduced ranges.**

1199 These results were calculated using spectrographic cross-correlation similarity. The means
1200 and 95% confidence intervals (CIs) were obtained by summarizing across 100 resampling
1201 iterations for each of the 6 total bin numbers. The calculation used to report results in the
1202 main text (16 bins) is shown as a red "X". The 95% CIs are small and are not visible around
1203 the mean.

1204

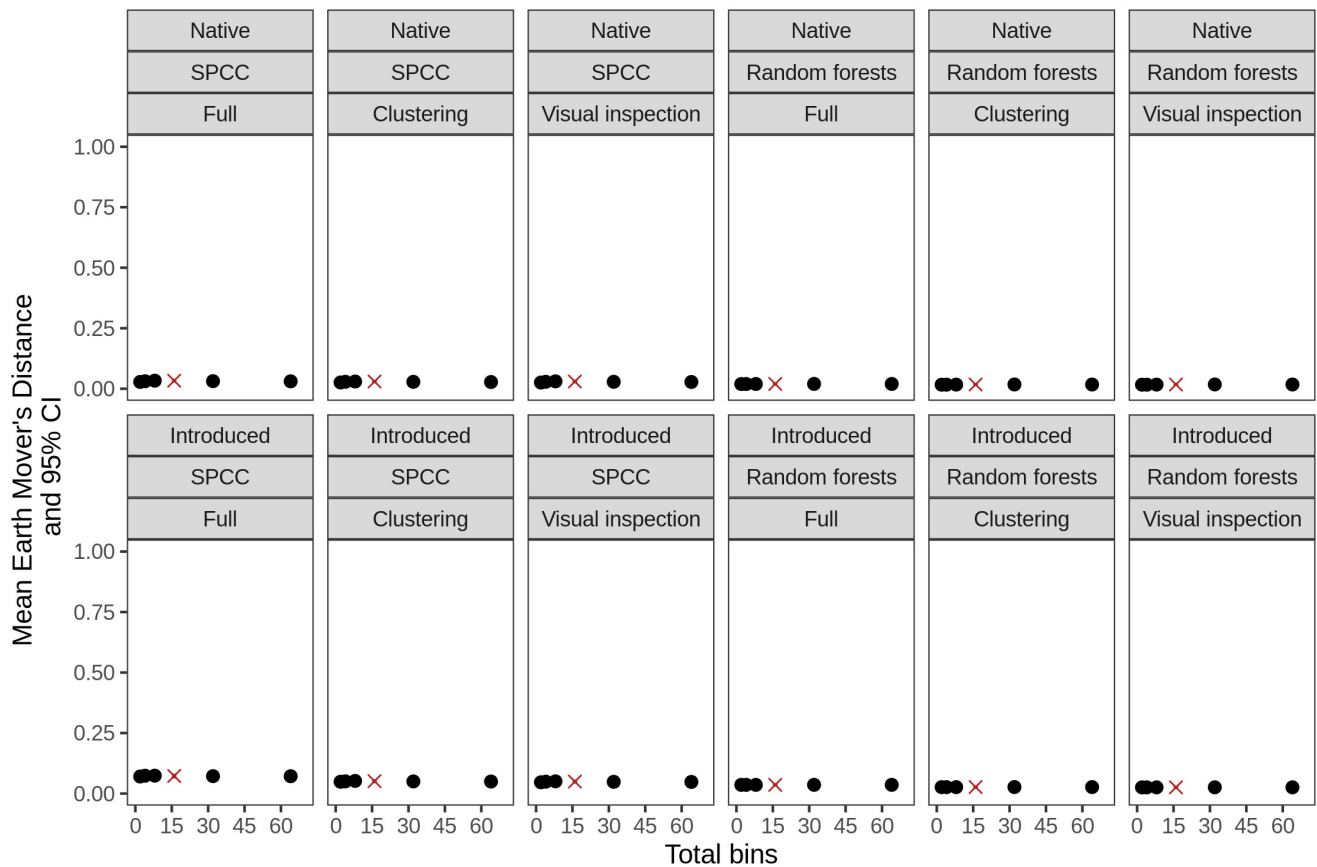
1205



1206 **S4 Fig. Earth Mover's Distance site scale results were consistent across total bin**
1207 **numbers in each of the native and introduced ranges.**

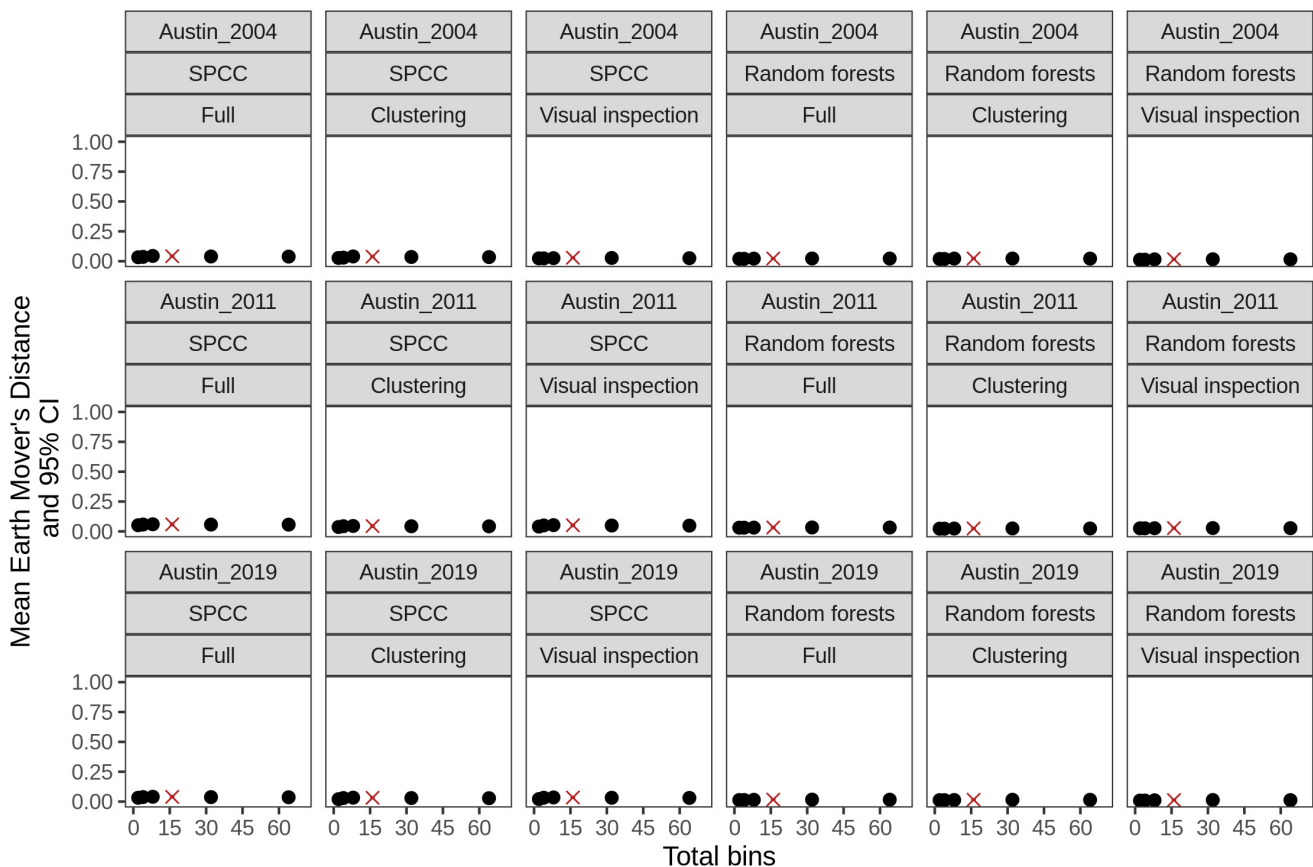
1208 These results were generated using spectrographic cross-correlation and random forests
1209 similarity, as well as the three site scale datasets used to address repeated sampling of
1210 unmarked individuals. The means and 95% confidence intervals (CIs) were obtained by
1211 summarizing across 100 resampling iterations for each bin number. The calculation used to
1212 report results in the main text (16 bins) is shown as a red "X". The 95% CIs are small and are
1213 not visible around the mean.

1214

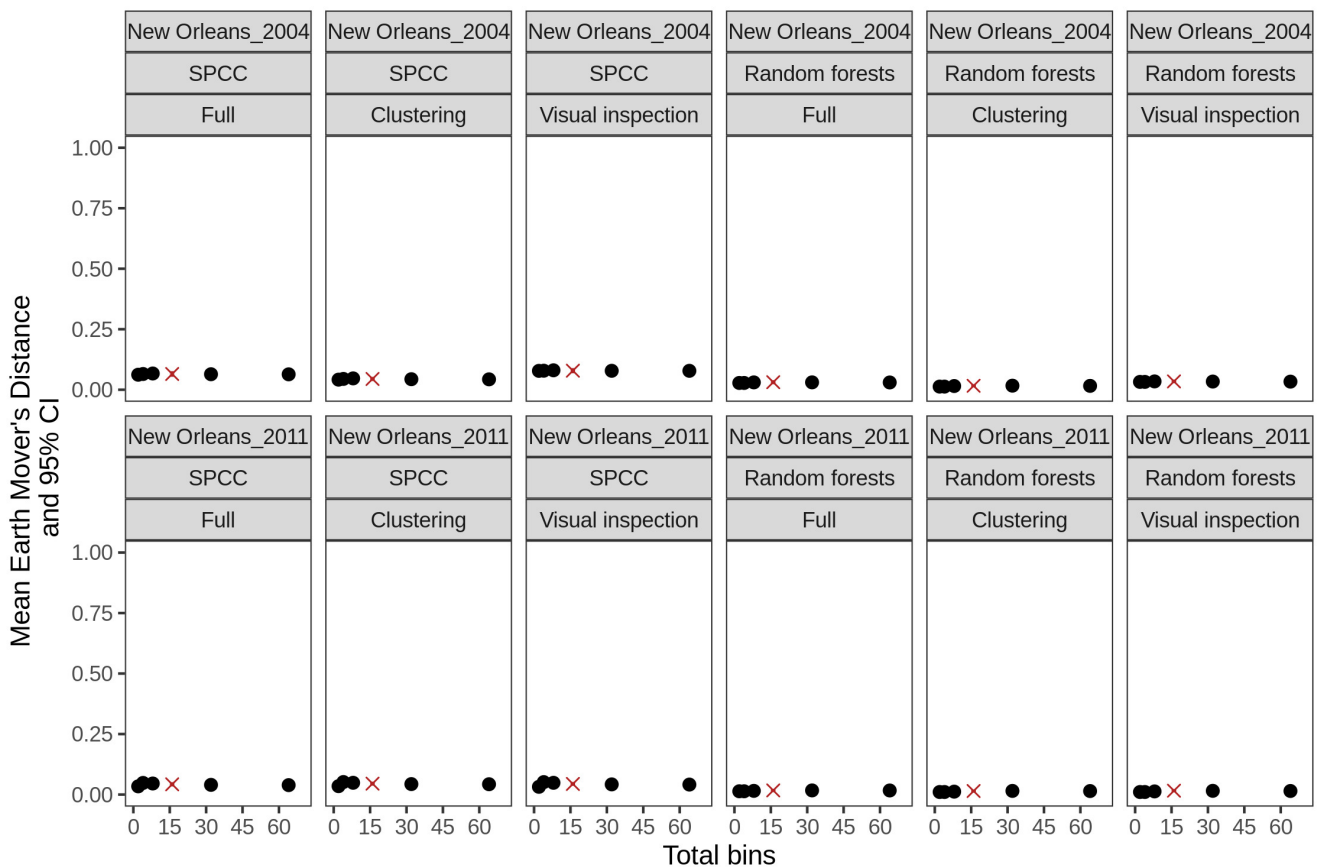


1216 **S5 Fig. Earth Mover's Distance site scale results were consistent across total bin**
 1217 **numbers over 3 sampling years for Austin, TX (in the U.S. introduced range).**

1218 These results were generated using spectrographic cross-correlation and random forests
 1219 similarity, as well as the three site scale datasets used to address repeated sampling of
 1220 unmarked individuals. The means and 95% confidence intervals (CIs) were obtained by
 1221 summarizing across 100 resampling iterations for each bin number. The calculation used to
 1222 report results in the main text (with 16 bins) is shown as a red "X". These 95% CIs are also
 1223 small and are not visible around the mean.



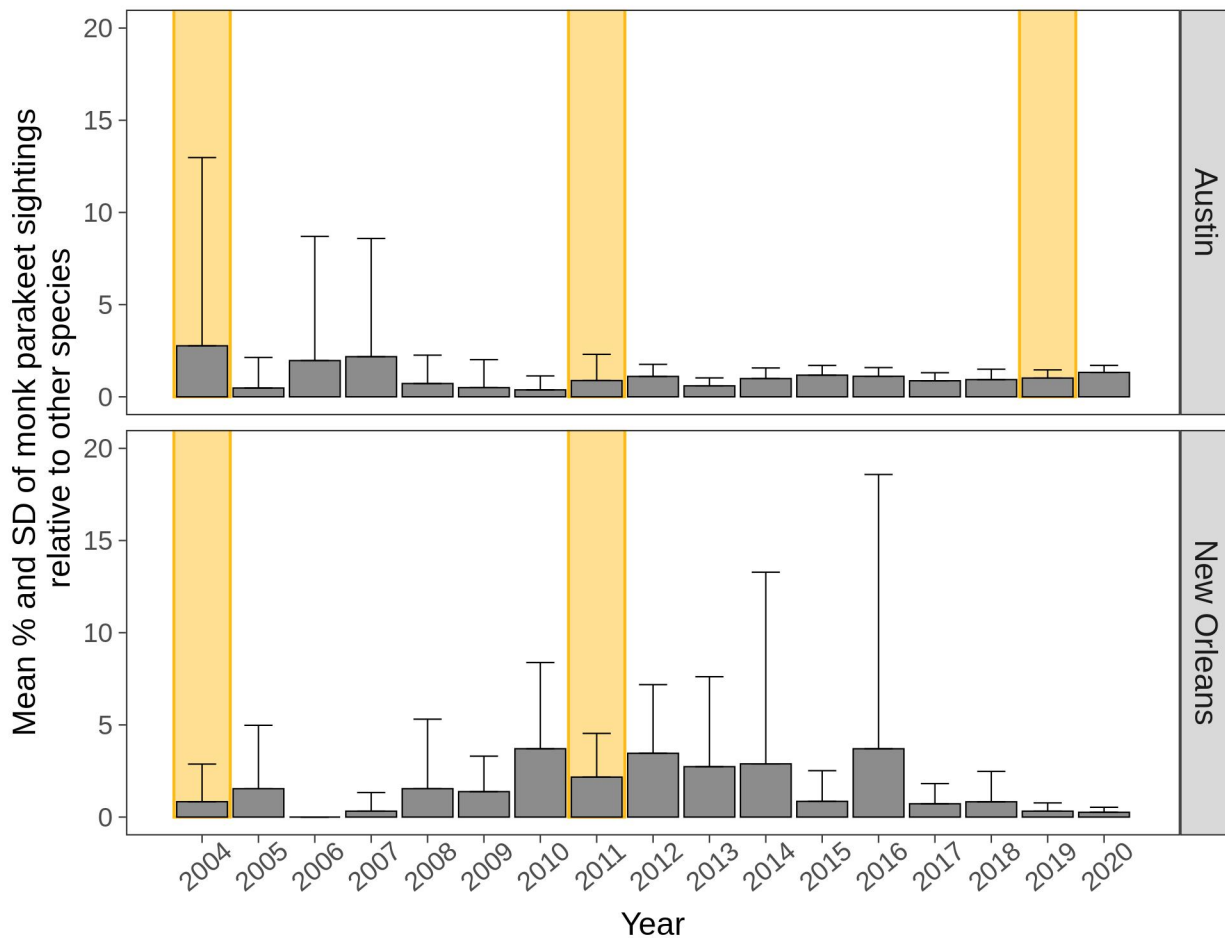
1225 **S6 Fig. Earth Mover's Distance site scale results were consistent across total bin**
 1226 **numbers over 2 sampling years for New Orleans, LA (in the U.S. introduced range).**
 1227 These results were generated using spectrographic cross-correlation and random forests
 1228 similarity, as well as the three site scale datasets used to address repeated sampling of
 1229 unmarked individuals. The means and 95% confidence intervals (CIs) were obtained by
 1230 summarizing across 100 resampling iterations for each bin number. As above, the calculation
 1231 used to report results in the main text (with 16 bins) is shown as a red "X", and the 95% CIs
 1232 are not visible around the mean.
 1233



1235 **S7 Fig. The frequency of introduced range monk parakeet sightings relative to other**
1236 **species reported in complete eBird checklists remained low over our sampling years in**
1237 **Austin and New Orleans (2004 to early 2020).**

1238 Each bar represents the mean percentage of monk parakeets observed relative to other
1239 species, averaged across weeks per year. The error bars denote the standard error. Gold
1240 rectangles highlight the sampling years in which monk parakeets were recorded in each city.

1241



1242 **S8 Fig. Density curves of spectrographic cross-correlation (SPCC) values for monk**
1243 **parakeets and yellow-naped amazons, as well as an acoustic space plot for yellow-**
1244 **naped amazons.**

1245 Panels A, B, and C show density curves of SPCC values for native range monk parakeets,
1246 introduced range monk parakeets, and yellow-naped amazons, respectively. Each density
1247 curve was generated from the full symmetric matrix of similarity values for the given species
1248 and range (including the diagonal). Panel D shows acoustic space for yellow-naped amazon
1249 contact calls, and points are colored by three regional dialects reported in Costa Rica by
1250 [23] (Nor = North, Nic = Nicaragua, Sou = South). We used these graphics to doublecheck the
1251 similarity values that we used for our comparative analysis.

